

Metapopulation dynamics on the brink of extinction

A. Eriksson^a, F. Elías-Wolff^b, B. Mehlig^b

^a*Department of Zoology, University of Cambridge, Cambridge, CB2 3EJ, UK*

^b*Department of Physics, University of Gothenburg, SE-41296 Gothenburg, Sweden*

Abstract

We analyse metapopulation dynamics in terms of an individual-based, stochastic model of a finite metapopulation. We suggest a new approach, using the number of patches in the population as a large parameter. This approach does not require that the number of individuals per patch is large, neither is it necessary to assume a time-scale separation between local population dynamics and migration. Our approach makes it possible to accurately describe the dynamics of metapopulations consisting of many small patches. We focus on metapopulations on the brink of extinction. We estimate the time to extinction and describe the most likely path to extinction. We find that the logarithm of the time to extinction is proportional to the product of two vectors, the vector of patch abundances in the quasi-steady state, and a vector – related to Fisher’s reproduction vector – that quantifies the sensitivity of the quasi-steady state distribution to demographic fluctuations. We compare our analytical results to stochastic simulations of the model, and discuss the range of validity of the analytical expressions. By identifying fast and slow degrees of freedom in the metapopulation dynamics, we show that the dynamics of large metapopulations close to extinction is approximately described by an effective deterministic equation originally proposed by Levins (1969). We were able to compute the rates in Levins’ equation in terms of the parameters of our stochastic, individual-based model. It turns out, however, that the interpretation of the dynamical variable depends strongly on the intrinsic growth rate and carrying capacity of the patches. Only when the carrying capacity is large does the slow variable correspond to the number of patches, as envisaged by Levins. Last but not least, we discuss how our findings relate to other, widely used metapopulation models.

Keywords: Metapopulations, stochastic dynamics, extinction, migration

1. Introduction

The habitats of animal populations are often geographically divided into many small patches, either because of human interference or because natural habitats are patchy. Understanding the dynamics of such populations is a problem of great theoretical and practical interest. Isolated small patches are often extinction prone, for example because of inbreeding in combination with demographic and environmental stochasticity (Hanski, 1999). When the patches are connected into a network by migration, local populations may still be prone to extinction, but the whole population may persist because empty patches are recolonised by migrants from surrounding occupied patches. Moreover, when the migration rate is sufficiently large, local populations can be stabilised by an inflow of immigrants (the rescue effect). Given a model of such a population, the main concern is usually to find out how the different parameter values in the model affect the growth and persistence of the metapopulation.

In Levins' model, the metapopulation dynamics is simplified by treating each patch as either occupied or empty (Levins, 1969). The rates of patch colonisation and extinction are expressed as functions of the total fraction of occupied patches in the population. In its simplest form Levins' model describes the time change of the fraction Q of occupied patches:

$$\frac{dQ}{dt} = c Q(1 - Q) - e Q. \quad (1)$$

Here c is the rate of successful colonisation of an empty patch, and e is the rate at which occupied patches turn empty (the rate of patch extinction). Both rates are effective parameters. How they are related to the microscopic rates determining the stochastic, individual-based metapopulation dynamics is not known. In spatially explicit models the parameters are chosen to be functions of for example the number of neighbouring patches (Hui and Li, 2004; Roy et al., 2008). Eq. (1) is generally motivated by assuming a separation of time scales between colonisation and extinction of patches on the one hand, and the population dynamics within the patches on the other hand (Levins, 1969; Hanski and Gyllenberg, 1993; Lande et al., 1998; Etienne, 2002). Many of the mechanisms that can be observed in natural populations (e.g. Allee and rescue effects) can be represented by suitable modifications of Eq. (1), and the qualitative behaviour of such models is well understood (Hanski and Ovaskainen, 2000; Etienne, 2000; Harding and McNamara, 2002; Zhou and Wang, 2004). See also Zhou et al. (2004); Taylor and Hastings (2005), and Martcheva and Bolker (2007).

Models that describe the metapopulation dynamics in terms of the fraction of occupied patches exhibit no explicit connection to the population dynamics within each patch, i.e. it is not apparent how individual births, deaths, or migration events translate into effective colonisation and extinction rates (Etienne, 2002). An alternative line of analysis focuses on the population dynamics within a single patch (Drechsler and Wissel, 1997; Lopez and Pfister, 2001). The advantage of this approach is that birth and death processes, emigration and immigration, can be modeled explicitly in terms of the number of individuals in the patch. This makes the model much more immediate in terms of biological processes (such as density dependence and Allee effects), but the rest of the metapopulation is reduced to a background source of immigrants (assumed to be stationary) and is not explicitly modeled.

Several authors have attempted to bridge the gap between detailed local population dynamics and the dynamics at the overall population level. Chesson (1981, 1984), Hanski and Gyllenberg (1993), Casagrandi and Gatto (1999, 2002), Nachman (2000) and others have analysed the equilibrium states and possible persistence of metapopulations in a model consisting of infinitely many patches with local dynamics coupled via a migration pool. The assumption that there are infinitely many patches is crucial in these studies, as it makes it possible to pose the question under which circumstances the metapopulation persists *ad infinitum*, that is for which choice of parameters the metapopulation dynamics reaches a non-trivial stable equilibrium. For finite metapopulations, by contrast, there is no stable equilibrium corresponding to persistence. As is well known, finite populations must eventually become extinct (unless they continue to grow). This fact is referred to as the ‘merciless dichotomy of population dynamics’ by Jagers (1992).

In this paper we characterise the dynamics of metapopulations with a large, but finite, number of patches. We derive, from first principles, how the global stochastic dynamics leads to an effective time evolution of the distribution of individuals over patches. The only critical assumption in our derivation is that the number of patches is large enough. Especially, it is not necessary to assume that the typical number of individuals per patch is large. Neither is it necessary to assume a time-scale separation between local and migration dynamics. We show that our results represent the typical transient of the metapopulation towards a quasi-steady state (if such a state exists).

On the brink of extinction, that is close to the bifurcation point where an infinite metapopulation ceases to persist, we use a systematic expansion of the exact Master equation in powers of N^{-1} (where N is the number of patches) to find the most likely path to extinction, as well as the leading contribution to the time

to extinction. In this case (close to the bifurcation) the metapopulation dynamics simplifies considerably: we show that it can be approximated by a simple, one-dimensional dynamics. This fact is a consequence of a general principle (Guckenheimer and Holmes, 1983) stating that a dynamical system close to a bifurcation exhibits a ‘slow mode’: a particular linear combination of the dynamical variables is found to relax slowly, the remaining degrees of freedom relax much more quickly and may be assumed to be in local equilibria. This renders the dynamics effectively one-dimensional. We find the slow mode of the metapopulation dynamics and show how it depends on the properties of the local dynamics (given by the local growth rate and the local carrying capacity). The slow mode determines the stochastic dynamics of finite metapopulations as well as the deterministic dynamics of metapopulations consisting of infinitely many patches. In the latter case we find that the slow mode obeys Eq. (1). We derive how the effective parameters c and e depend on the local population dynamics. It turns out that the variable Q is in general not given by the fraction of occupied patches as envisaged by Levins. But we show that Q approaches the fraction of occupied patches in the limit of large patch carrying capacities and large local growth rates (this is the limit of time-scale separation). In other words, we have succeeded in deriving Levins’ model, (1), from a stochastic, individual-based model of a finite metapopulation. We find that (1) is still valid (close to the bifurcation) even when there is no time-scale separation between the local and the migration dynamics. This is the consequence of the existence of a slow mode.

Lande et al. (1998) have suggested an elegant stochastic generalisation of Levins’ model, in an attempt to compute how the local patch dynamics affects the properties of the quasi-steady state of the metapopulation (and the average time to extinction of this population). Their main idea is to connect the extinction and colonisation rates to local processes. The extinction rate is calculated as the inverse expected time to extinction of a single patch at the carrying capacity (which is determined self-consistently), and colonisation is defined as the rate of a single migrant arriving to an empty patch, seeding a population that grows to the carrying capacity. This scheme is persuasive but not rigorous. The predictions of Lande et al. (1998) have, to our knowledge, never been tested by comparisons to results of simulations of stochastic, individual-based metapopulation models. Therefore it is important that our approach allows us to compute the rates of extinction and colonisation from first principles. In the limit of large patch carrying capacities and close to the bifurcation we obtain expressions (exact in the limit we consider) that are very similar, but not identical, to the relations proposed by Lande et al. (1998).

In summary, we have characterised the stochastic dynamics of metapopulations on the brink of extinction. Using an expansion of the exact Master equation describing the stochastic dynamics with the number N of patches as a large parameter, we were able to identify a slow mode in the metapopulation dynamics, regardless of whether there is a time-scale separation between local and global dynamics or not. We could show under which circumstances widely used effective metapopulation models provide accurate descriptions of metapopulation dynamics.

The remainder of this paper is organised as follows. In section 2 we describe the individual-based stochastic metapopulation model investigated here. We summarise how our numerical experiments were performed and briefly describe how to represent the metapopulation dynamics in terms of a Master equation, and how to expand this equation in powers of N^{-1} . Our results are described in section 3. We first discuss the limit $N \rightarrow \infty$ and discuss under which circumstances metapopulations persist in this limit. We then analyse the metapopulation dynamics in this limit. Second, we turn to stochastic fluctuations of finite metapopulations, and summarise our results on fluctuations in the quasi-steady state, the most likely path to extinction as well as the average time to extinction. Section 4 contains our conclusions.

2. Methods

In this section we define the stochastic, individual-based metapopulation model that is analysed in this paper. We describe how our numerical experiments are performed and derive a Master equation, Eq. (13), that is the starting point for our mathematical analysis of metapopulation dynamics. In general it is not possible to solve this equation in closed form. We demonstrate how an approximate solution can be obtained by expanding the Master equation using the number N of patches as a large parameter. In the limit of $N \rightarrow \infty$, the dynamics reduces to a deterministic model. The equilibrium properties of this model were analysed by Casagrandi and Gatto (1999, 2002), and by Nachman (2000).

2.1. Stochastic, individual-based metapopulation model

The model consists of a population distributed amongst N patches, as illustrated in Fig. 1. In each patch, the local population dynamics is a birth-death process with birth rates b_i , and death rates d_i . Here i denotes the population size in a given patch (and $b_0 = d_0 = 0$). To simplify the discussion we assume that the rates are the same for all patches, but more general cases can be treated within the

approach described in this paper. In the following we illustrate our results for a particular choice of birth and death rates:

$$b_i = r i \quad \text{birth rate ,} \quad (2)$$

$$d_i = \mu i + (r - \mu)i^2/K \quad \text{death rate .} \quad (3)$$

The parameter r is the birth rate per individual, μ is the density-independent per capita mortality, and K determines the carrying capacity of a single patch. For simplicity, we take $\mu = 1$ hereafter (this corresponds to measuring time in units of the expected life-time of individuals in the absence of density dependence).

In addition to the local population dynamics, the number of individuals in each patch can change because some individuals emigrate from their patch to other patches, or because immigrants arrive from other patches.

Following Hanski and Gyllenberg (1993), the migration process is modeled as follows: individuals emigrate from a patch at rate m_i , where i is the population size on the patch in question ($m_0 = 0$). If the individuals migrate independently and with constant rates, m_i is proportional to i :

$$m_i = m i \quad \text{emigration rate .} \quad (4)$$

More complex migration patterns can be incorporated. If for example individuals moved to avoid overcrowding, the migration rate would be density dependent. The emigrants enter a common dispersal pool, containing the migrants from all patches that have not yet reached their target patch. Each migrant stays an exponentially distributed time in the pool, with expected value $1/\alpha$, before reaching the target habitat, which is chosen with equal probability among all patches. This process is illustrated in Fig. 1. Migration may fail if the individuals die before reaching the new habitat; this is modeled by the rate ν of dying per unit of time during dispersal. In practice, the probability of successful migration depends on the background mortality of the individuals, on the time it spends in the dispersal pool, and on additional perils individuals may be exposed to during dispersal (e.g. increased risk of predation due to lack of cover, etc.). Thus, if there are M migrants, $(\alpha + \nu)M$ individuals leave the dispersal pool per unit of time, and the rate of immigration to a given patch is $I = \alpha M/N$.

2.2. Numerical experiments

In the direct numerical simulations, the population is evolved in the following manner. First, at any given time, the local rates (2-4) sum to a rate of the next

locally generated event, Λ_k . If patch k contains i individuals

$$\Lambda_k = b_i + d_i + m_i. \quad (5)$$

The sum of these rates over all patches, $\Lambda = \sum_k \Lambda_k$ for $k = 1, \dots, N$, yields the rate for the next event occurring in the population. Thus the simulation proceeds by generating an exponentially distributed random number with expected value $1/\Lambda$. Second, at each time step, a patch is chosen with probability Λ_k/Λ . Third, the type of event is chosen randomly: birth with probability b_i/Λ_k , death with probability d_i/Λ_k or emigration with m_i/Λ_k . Fourth, the numerical experiments described below were performed in the limit $\alpha \rightarrow \infty$ and for $\nu = 0$. This means that emigrating individuals are immediately assigned to a randomly chosen patch (possibly the one they come from).

2.3. Master equation

A natural and commonly adopted approach to describe stochastic population dynamics is to derive a Master equation (van Kampen, 1981) for the change in time of the probability ρ of observing i_1 individuals on the first patch, i_2 individuals on the second patch, \dots , and of observing M individuals in the migrant pool. Recently this approach was adopted by Meerson and Sasorov (2011) describing the dynamics of local birth-death processes coupled by nearest-neighbour interactions (diffusion).

In the following we pursue a different approach. Since the local population dynamics is assumed to be the same within all patches, it is sufficient to count the number of patches with a given number of individuals rather than keeping track of the number of individuals in each patch. Let n_j denote the number of patches with j inhabitants at a given time. The state of the population is described by the variables n_0, n_1, \dots , and M . We find the Master equation for the probability $\rho(n_0, n_1, \dots, M; t)$ by considering all possible transitions between the states of the population, contributing to the change of $\rho(n_0, n_1, \dots, M; t)$. Consider for instance the birth of an individual. A birth on a patch of size j (that is a patch with j individuals) corresponds to the transition $n_j + 1 \rightarrow n_j$ and $n_{j+1} - 1 \rightarrow n_{j+1}$ giving rise to the change

$$b_j(n_j + 1)\rho(\dots, n_j + 1, n_{j+1} - 1, \dots, M; t) - b_j n_j \rho(\dots, n_j, n_{j+1}, \dots, M; t) \quad (6)$$

in $\rho(n_0, n_1, \dots, M; t)$ per unit time. We write this contribution in terms of raising and lowering operators \mathbb{E}_j^\pm , defined by their effects on an arbitrary function (van Kampen, 1981):

$$\mathbb{E}_j^+ g(\dots, n_j, \dots) = g(\dots, n_j + 1, \dots), \quad \mathbb{E}_j^- g(\dots, n_j, \dots) = g(\dots, n_j - 1, \dots). \quad (7)$$

Adopting this notation, the contribution (6) equals

$$(\mathbb{E}_j^+ \mathbb{E}_{j+1}^- - 1) b_j n_j \rho. \quad (8)$$

Adding up the contributions due to death, emigration, and immigration we find:

$$\begin{aligned} \frac{\partial \rho}{\partial t} = & \sum_{j=0}^{\infty} (\mathbb{E}_j^+ \mathbb{E}_{j+1}^- - 1) b_j n_j \rho \\ & + \sum_{j=0}^{\infty} (\mathbb{E}_j^+ \mathbb{E}_{j-1}^- - 1) d_j n_j \rho + \sum_{j=0}^{\infty} (\mathbb{E}_j^+ \mathbb{E}_{j-1}^- \mathbb{E}_M^- - 1) m_j n_j \rho \\ & + \sum_{j=0}^{\infty} (\mathbb{E}_j^+ \mathbb{E}_{j+1}^- \mathbb{E}_M^+ - 1) \alpha M \frac{n_j}{N} \rho + (\mathbb{E}_M^+ - 1) \nu M \rho. \end{aligned} \quad (9)$$

To simplify the discussion we assume that migration is instantaneous, this corresponds to taking the limit $\alpha \rightarrow \infty$ and $\nu = 0$. In this limit, the immigration rate to a patch is given by:

$$I = \frac{1}{N} \sum_{j=0}^{\infty} m_j n_j, \quad (10)$$

and the corresponding Master equation takes the form:

$$\begin{aligned} \frac{\partial \rho}{\partial t} = & \sum_{j=0}^{\infty} (\mathbb{E}_j^+ \mathbb{E}_{j+1}^- - 1) b_j n_j \rho + \sum_{j=0}^{\infty} (\mathbb{E}_j^+ \mathbb{E}_{j-1}^- - 1) d_j n_j \rho \\ & + \frac{1}{N} \sum_{i=1}^{\infty} \sum_{j=0}^{\infty} (\mathbb{E}_{i-1}^- \mathbb{E}_i^+ \mathbb{E}_j^+ \mathbb{E}_{j+1}^- - 1) m_i n_i n_j \rho. \end{aligned} \quad (11)$$

Here only terms of lowest order in N^{-1} were kept. The last term on the right-hand side of Eq. (11) describes instantaneous migration where $M = 0$.

The number of patches is given by $N = \sum_{j=0}^{\infty} n_j$. The following discussion is simplified by making this constraint explicit in the Master equation (11). This is achieved by considering n_0 , the number of empty patches, to be a function of n_1, n_2, \dots :

$$n_0 = N - \sum_{j=1}^{\infty} n_j. \quad (12)$$

Using (12) we find the following Master equation:

$$\begin{aligned}
\frac{\partial \rho(\mathbf{n}, t)}{\partial t} = & \sum_{j=0}^{\infty} (\mathbb{E}_j^+ \mathbb{E}_{j+1}^- - 1) b_j n_j \rho(\mathbf{n}, t) + \sum_{j=0}^{\infty} (\mathbb{E}_j^+ \mathbb{E}_{j-1}^- - 1) d_j n_j \rho(\mathbf{n}, t) \\
& + \frac{1}{N} \sum_{i=1}^{\infty} \sum_{j=1}^{\infty} (\mathbb{E}_{i-1}^- \mathbb{E}_i^+ \mathbb{E}_j^+ \mathbb{E}_{j+1}^- - 1) m_i n_i n_j \rho(\mathbf{n}, t) \\
& + \sum_{i=1}^{\infty} (\mathbb{E}_{i-1}^- \mathbb{E}_i^+ \mathbb{E}_1^- - 1) m_i n_i \left(1 - \frac{1}{N} \sum_{j=1}^{\infty} n_j\right) \rho(\mathbf{n}, t).
\end{aligned} \tag{13}$$

Here the components n_j of the vector $\mathbf{n} = (n_1, n_2, \dots)^\top$ denote the number of patches with $j \geq 1$ individuals, and $\mathbb{E}_0^\pm \equiv 1$. Eq. (13) describes the stochastic population dynamics of the metapopulation model considered here. In principle, (13) can be integrated explicitly. In practice, however, because the number of possible configurations grows exponentially with the number of patches, it is not possible to use the full Master equation (9) except when the number of patches and the maximum population size are both small.

In the next section we describe the approximate method of solving (13) adopted in the following. It corresponds to a systematic expansion of the Master equation, using the number N of patches in the population as a large parameter. This approach does not require that the number of individuals per patch is large, neither is it necessary to assume a time-scale separation between local population dynamics and migration. Our approach makes it possible to accurately describe the dynamics of metapopulations consisting of many small patches. In the limit of infinitely many patches, to lowest order in the expansion, a deterministic metapopulation dynamics is obtained. Stochastic fluctuations in metapopulations with a large but finite number of patches are described by the leading order of the expansion.

2.4. Expansion of the Master equation

When the number N of patches is sufficiently large (so that the total population size is large, even though the number of individuals per patch may be small), the following approach can be used to approximately describe the metapopulation dynamics. When N is large we expect that the probability ρ of observing a given distribution of \mathbf{n} changes only little when patches change in population size. It is important to emphasize that no assumption is made concerning the size of the changes to the population size of any single habitat. It is merely assumed that there are sufficiently many patches that they form a statistical ensemble. Hence,

on the level of the meta population, this leads only to a single increment and decrement in the count of the number of patches with a given number of individuals. For instance, it is perfectly possible to have big jumps in the population sizes of individual patches in the model without violating the assumption that the distribution of \mathbf{n} is smooth, and to allow the local population dynamic to depend sensitively on the patch abundance when there are few individuals in the patch (for example, modeling the effect of abundance on mating success (Sæther et al., 2004; Melbourne and Hastings, 2008)). It is convenient to express the patch population sizes \mathbf{n} in terms of the scaled frequency $f_j = n_j/N$. The probability $\tilde{\rho}$ of observing f_1, f_2, \dots is related to the probability ρ by

$$\tilde{\rho}(\mathbf{f}; t) = \rho(N\mathbf{f}; t). \quad (14)$$

In contrast to the distribution of n_j , the distribution of f_j is expected to become approximately independent of N for a large number of patches. A change of a single count n_j leads only to a change of $1/N$ in f_j . Since the probability $\tilde{\rho}$ is an approximately continuous function of f_j in the limit of large values of N , we seek an approximate solution of (13) by expanding this equation in powers of N^{-1} .

In the limit of $N \rightarrow \infty$ we expect that stochastic fluctuations are negligible, so that the metapopulation dynamics becomes deterministic. It takes the form of a kinetic equation for \mathbf{f} :

$$\frac{d\mathbf{f}}{dt} = \mathbf{v}(\mathbf{f}). \quad (15)$$

In this limit, the question whether or not the metapopulation may persist is answered by finding the steady states \mathbf{f}^* of the system (15), given by $\mathbf{v}(\mathbf{f}^*) = 0$. Persistence corresponds to the existence of a stable steady state with positive components $f_j^* > 0$ for some values of j . If, by contrast, the only stable steady state is $\mathbf{f}^* = 0$, then the metapopulation will definitely become extinct. The time to extinction is determined by (15) and the initial conditions.

For large (but finite) values of N the metapopulation fluctuates around the stable steady states \mathbf{f}^* of (15). These fluctuations can be described by expanding the Master equation (13) to leading order in N^{-1} . The stochastic fluctuations are expected to be small when N is large, but they are crucial to the metapopulation dynamics as mentioned in the introduction. When the number of patches is finite, the metapopulation must eventually become extinct (the state $\mathbf{f} = 0$ is the only absorbing state of the Master equation). When N is large, the time to extinction from a stable steady state of the deterministic dynamics is expected to be large. By analogy with standard large-deviation analysis we expect that the time

to extinction increases exponentially with increasing N , giving rise to a long-lived quasi-steady state. Below we analyse its properties in order to estimate the time to extinction. Our result is consistent with the above expectation, and we show that the time to extinction depends sensitively on the parameters of the model (r, K, m , and N).

2.4.1. Deterministic dynamics in the limit of $N \rightarrow \infty$

To simplify the notation, we drop the tilde in (14) so that $\rho(\mathbf{f}, t)$ is the probability of observing, at time t , a fraction f_1 of patches with one individual, a fraction f_2 of patches with two individuals, and so forth. In deriving the expansion of the Master equation (13) we use the approach described by van Kampen (1981). Assuming that ρ is a smooth function of \mathbf{f} , the action of the raising and lowering operators (7) act on ρ approximately as

$$\mathbb{E}_j^\pm = \exp(\pm N^{-1} \partial_{f_j}). \quad (16)$$

The Master equation (13) is expanded as follows. We replace n_j by Nf_j in (13), insert (16), and expand in powers of N^{-1} . Keeping only the lowest order in N^{-1} , we arrive at a transport equation for ρ that corresponds to deterministic dynamics of the form (15). We find that the components of $\mathbf{v}(\mathbf{f})$ are given by:

$$\begin{aligned} v_j(\mathbf{f}) &= (b_{j-1} + I)f_{j-1} + (d_{j+1} + m_{j+1})f_{j+1} - (b_j + I + d_j + m_j)f_j \quad \text{for } j > 1, \\ v_1(\mathbf{f}) &= I(1 - \sum_{k=1}^{\infty} f_k) + (d_2 + m_2)f_2 - (b_1 + I + d_1 + m_1)f_1. \end{aligned} \quad (17)$$

Here $I = \sum_{k=1}^{\infty} m_k f_k$ is the rate of immigration into a given patch, corresponding to (10). Since I depends upon \mathbf{f} , the deterministic dynamics (15,17) is nonlinear. We note that Eqs. (15,17) correspond to the metapopulation model suggested by Casagrandi and Gatto (1999) and Nachman (2000). Here we have derived it by a systematic expansion of the exact Master equation in powers of N^{-1} where N is the number of patches. Our derivation emphasises the fact that (15,17) approximate the metapopulation dynamics by a deterministic equation. Arrigoni (2003) has shown that this limit holds under quite general assumptions for the underlying stochastic model. Casagrandi and Gatto (1999), Nachman (2000), and others have studied how the stability of the steady states of the deterministic model (15,17) depend upon the parameters of the model. However, (15,17) cannot be used to determine how stochastic population dynamics affects metapopulation persistence. In order to take the stochastic fluctuations into account, it is necessary to consider the next higher order in $1/N$.

2.4.2. Quasi-steady state distribution at finite but large values of N

Metapopulations consisting of a finite but large number of patches exhibit stochastic fluctuations around the stable steady states \mathbf{f}^* of the deterministic dynamics (15). For large values of N , these fluctuations are expected to be small. But as explained above, extinction is certain, although the metapopulation may persist for an exponentially long time. This leads to a quasi-stable steady state. We analyse its properties by expanding the Master equation to leading order in N^{-1} , using a standard method that is referred to as WKB analysis (Wilkinson et al., 2007), as the eikonal approximation (Dykman et al., 1994), or as the large-deviation principle (Freidlin and Wentzell, 1984) in the mathematical literature.

We briefly outline this method in the remainder of this subsection. For a comprehensive description, the reader is referred to Altland and Simons (2010), Elgart and Kamenev (2004), and Dykman et al. (1994). In the quasi-steady state we expect $d\rho/dt \approx 0$ and seek a solution of the Master equation of the form

$$\rho(\mathbf{f}) \approx \exp[-NS(\mathbf{f}) + \text{higher orders in } N^{-1}]. \quad (18)$$

The function $S(\mathbf{f})$ is commonly referred to as the ‘action’. It is convenient to define it such that $S(\mathbf{f}^*) = 0$. In the vicinity of the steady state we expect the distribution $\rho(\mathbf{f})$ to be Gaussian, and thus $S(\mathbf{f})$ to be a quadratic function of $\mathbf{f} - \mathbf{f}^*$. In order to characterise the extinction dynamics of the metapopulation, it is necessary to determine the tails of this distribution, corresponding to large deviations of \mathbf{f} from \mathbf{f}^* . This is achieved by inserting the ansatz (18) into the Master equation (13), making use of (16), and expanding in N^{-1} . One finds a first-order partial differential equation for $S(\mathbf{f})$:

$$H\left(\mathbf{f}, \frac{\partial S(\mathbf{f})}{\partial \mathbf{f}}\right) = 0. \quad (19)$$

In our case, for the Master equation (13), we obtain:

$$\begin{aligned} H(\mathbf{f}, \mathbf{p}) = & \sum_{j=0}^{\infty} (e^{p_{j+1}-p_j} - 1) b_j f_j + \sum_{j=0}^{\infty} (e^{p_{j-1}-p_j} - 1) d_j f_j \\ & + \sum_{i=1}^{\infty} \sum_{j=1}^{\infty} (e^{p_{i-1}-p_i-p_j+p_{j+1}} - 1) m_i f_i f_j \\ & + \sum_{j=1}^{\infty} (e^{p_{j-1}-p_j+p_1} - 1) m_j f_j \left(1 - \sum_{k=1}^{\infty} f_k\right). \end{aligned} \quad (20)$$

Here $\mathbf{p} = (p_1, p_2, \dots)^\top$, $p_j = \partial S / \partial f_j$ for $j \geq 1$, and $p_0 = 0$. The solution of (19,20) is found by recognising that (19) is a Hamilton-Jacobi equation for an auxiliary classical Hamiltonian dynamics with configuration-space variables \mathbf{f} and ‘momenta’ \mathbf{p} :

$$\frac{d\mathbf{f}}{dt} = \frac{\partial H}{\partial \mathbf{p}}, \quad \text{and} \quad \frac{d\mathbf{p}}{dt} = -\frac{\partial H}{\partial \mathbf{f}}. \quad (21)$$

Now consider solutions of Eqs. (21) satisfying

$$\left. \begin{array}{l} \mathbf{f}(t) \rightarrow \mathbf{f}^* \\ \mathbf{p}(t) \rightarrow \mathbf{0} \end{array} \right\} \quad \text{as } t \rightarrow -\infty, \quad \mathbf{f}(t) \rightarrow \mathbf{f} \quad \text{as } t \rightarrow \infty, \quad \text{and} \quad H(\mathbf{f}(t), \mathbf{p}(t)) = 0. \quad (22)$$

To every such solution corresponds an action $S(\mathbf{f})$ obtained by integrating the momentum along the path $(\mathbf{f}(t), \mathbf{p}(t))$:

$$S(\mathbf{f}) = \int_{-\infty}^{\infty} dt \mathbf{p}^\top d\mathbf{f}/dt. \quad (23)$$

The boundary conditions (22) are motivated as follows. Observe that to each stable steady state \mathbf{f}^* of the deterministic dynamics (15) there corresponds a steady state $(\mathbf{f}^*, \mathbf{p}^* = \mathbf{0})$ of the auxiliary dynamics (21). This can be seen by expanding the function $H(\mathbf{f}, \mathbf{p})$ to second order in \mathbf{p} around $\mathbf{p} = \mathbf{0}$

$$H(\mathbf{f}, \mathbf{p}) = \mathbf{p}^\top \mathbf{v}(\mathbf{f}) + \frac{1}{2} \mathbf{p}^\top \mathbf{D}(\mathbf{f}) \mathbf{p} + \dots. \quad (24)$$

Here $\mathbf{v}(\mathbf{f})$ is given by (17), and the symmetric matrix $\mathbf{D}(\mathbf{f})$ has elements $D_{ij} = \partial^2 H / \partial p_i \partial p_j$. The elements are given in appendix A. Eq. (24) shows that the auxiliary dynamics for $\mathbf{p} = 0$ corresponds to the deterministic dynamics given in Eq. (15). The stability of the steady state $(\mathbf{f}^*, \mathbf{0})$ is determined by the eigenvalues of the matrix

$$\mathbf{J} = \begin{pmatrix} \mathbf{A} & \mathbf{D} \\ \mathbf{0} & -\mathbf{A}^\top \end{pmatrix}. \quad (25)$$

The matrix $\mathbf{A}(\mathbf{f})$ has elements $A_{ij} = \partial v_i / \partial f_j$ evaluated at $\mathbf{f} = \mathbf{f}^*$. It is the stability matrix of the stable steady state \mathbf{f}^* of the deterministic dynamics (15). Its elements can be obtained from Eq. (A.2) in appendix A. Similarly, \mathbf{D} is evaluated at \mathbf{f}^* . Assuming that the steady state \mathbf{f}^* is stable, the eigenvalues λ_α of \mathbf{A} must have negative real parts. It turns out that the eigenvalues are in fact negative. We write $0 > \lambda_1 > \lambda_2 > \dots$. The eigenvalues of \mathbf{J} occur in pairs λ_α , and $-\lambda_\alpha$. The steady state $(\mathbf{f}^*, \mathbf{0})$ of (21) is thus a saddle. In other words, stochastic fluctuations allow

metapopulations consisting of a finite number of patches to escape from the steady state \mathbf{f}^* (that is stable in the limit $N \rightarrow \infty$). In general there are (infinitely) many escape paths satisfying the boundary conditions (22). Freidlin and Wentzell (1984) formulated a variational principle for the most likely escape path: in the limit of large values of N , the probability distribution (18) is dominated by the escape path to $\mathbf{f} = \mathbf{0}$ with extremal action (23).

In the case of our metapopulation model, the auxiliary dynamics (21) is infinite dimensional. It is therefore not possible, in general, to find the optimal escape path explicitly. In practice one may truncate the dynamics by only considering a finite number of variables \mathbf{f}_j (up to a maximal value of j_{\max}). This is expected to be a good approximation when j_{\max} is taken to be much larger than the carrying capacity K , since $\mathbf{f}_j \approx 0$ for $j \gg K$. In our subsequent analysis of the problem we make use of the fact that the auxiliary dynamics simplifies considerably in the vicinity of a bifurcation of the deterministic dynamics (Guckenheimer and Holmes, 1983; Dykman et al., 1994).

Near the steady state \mathbf{f}^* , the distribution (18) is expected to be Gaussian, as mentioned above. This corresponds to an action quadratic in $\delta\mathbf{f} = \mathbf{f} - \mathbf{f}^*$:

$$S(\mathbf{f}) \approx \frac{1}{2} \delta\mathbf{f}^\top \mathbf{C}^{-1} \delta\mathbf{f}. \quad (26)$$

The matrix \mathbf{C} , which is the covariance matrix of the distribution (18) multiplied by N , can be obtained from the linearised auxiliary dynamics (21). Using $\mathbf{p} = \partial S / \partial \mathbf{f}$ we have

$$\delta\mathbf{p} = \frac{\partial S}{\partial \delta\mathbf{f}} = \mathbf{C}^{-1} \delta\mathbf{f}. \quad (27)$$

According to Eq. (22), the dynamics must obey $H(\mathbf{f}(t), \mathbf{p}(t)) = 0$. It follows from (24) that the linearised dynamics satisfies this constraint provided

$$\mathbf{A}\mathbf{C} + \mathbf{C}\mathbf{A}^\top + \mathbf{D} = \mathbf{0}. \quad (28)$$

3. Results and Discussion

In this section we summarise our results for the population dynamics of the metapopulation model described in Section 2.1, using the expansion of the Master equation outlined in Section 2.4. This section is divided into two parts. We first discuss the limit of infinitely many patches. Second, we analyse the most likely path to extinction in finite metapopulations. We also summarise our results for the average time to extinction of the metapopulation, and demonstrate that it depends sensitively on upon the parameters of the model (r , K , m , and N).

3.1. Infinitely many patches

It was shown in Section 2.4 that in the limit of infinitely many patches, the metapopulation dynamics is described by the deterministic dynamics (15), corresponding to the model proposed by Casagrandi and Gatto (1999) and Nachman (2000). In this subsection we briefly summarise our results on the persistence and the relaxation behaviour of the metapopulation model introduced in section 2.1.

3.1.1. Metapopulation persistence in the limit of infinitely many patches ($N \rightarrow \infty$)

For sufficiently large migration rates m , the deterministic dynamics (15,17) has two viable steady states. The state $\mathbf{f} = \mathbf{0}$ is unstable, and there is a second steady state \mathbf{f}^* given by

$$f_j^* = f_0^* \prod_{k=1}^j \frac{b_{k-1} + I^*}{d_k + m_k} \quad (29)$$

where I^* is the rate of immigration into a patch in the steady state. Eq. (29) is most easily understood by recognising that the deterministic dynamics (15,17) takes the form of a Master equation for the probabilities f_j that a patch is occupied by j individuals. Eq. (29) is equivalent to Eqs. (5a,b) in (Nachman, 2000) and to Eqs. (5,6) in (Casagrandi and Gatto, 2002). In (29), the factor f_0^* is a normalisation factor (equal to the frequency of empty patches in the steady state) determined by the requirement that $f_0^* + \sum_{j=1}^{\infty} f_j^* = 1$. Note that the factors in the product in (29) depend upon the rate I^* . This gives rise to a self-consistency condition for the rate of immigration I^* in the steady state:

$$I^* = \sum_{j=1}^{\infty} m_j f_j^*. \quad (30)$$

The steady state (29) is stable provided the eigenvalues of \mathbf{A} (this matrix is introduced in the previous section and its elements are given in appendix A) have negative real parts. This is the case when the steady-state immigration rate I^* is larger than zero. The steady-state immigration rate is expected to decrease when the emigration rate decreases. Consider for instance decreasing m , defined in Eq. (4), while keeping all other parameters constant. As m approaches a critical value, m_c , we observe that $I^* \rightarrow 0$. At the same time all components of \mathbf{f}^* tend to zero, and $f_0^* \rightarrow 1$. Below this critical point, that is for $m < m_c$, the stable steady state ceases to exist (and $\mathbf{f} = \mathbf{0}$ turns stable). In the limit of infinitely many patches ($N \rightarrow \infty$), the persistence condition

$$m > m_c \quad (31)$$

ensures that a stable steady state with $f_j^* > 0$ exists, for some non-zero values of j . This persistence criterion for infinitely large metapopulations is equivalent to the criterion suggested by Chesson (1984) and re-derived by Casagrandi and Gatto (2002), namely that the metapopulation persists provided that the expected number of emigrants from a patch with initially one individual and into which emigration is excluded is greater than unity. In a slightly different form this principle is quoted by Hanski (1998), namely that the expected number of successful colonisation out of a given patch during its lifetime in an otherwise empty metapopulation should be larger than unity. We emphasise that this criterion (or any of the equivalent criteria, such as (31)) cannot be used to determine how stochastic fluctuations in finite metapopulations affect their persistence.

The critical value m_c is obtained by analysing the steady-state condition (30) for m close to m_c . We write $m = m_c(1 + \delta)$ and expand the steady-state immigration rate in powers of δ (note that I^* vanishes at $\delta = 0$):

$$I^* = I_1\delta + I_2\delta^2 + \dots \quad (32)$$

The constant I_1 is given in appendix B. Expanding (30), we find to lowest order in δ a condition for m_c :

$$d_1 = m_c \sum_{j=2}^{\infty} j \prod_{k=2}^j \frac{b_{k-1}}{d_k + m_c k}. \quad (33)$$

Fig. 2 shows how the solution m_c of Eq. (33) depends upon the carrying capacity K for the model introduced in section 2.1. The critical migration rate is shown as a solid red line in the left panel of Fig. 2. Above this line, a metapopulation consisting of an infinite number of patches persists. Expanding the condition (33) for large carrying capacities K we find that m_c decreases exponentially with increasing values of K (see appendix C):

$$m_c \sim r \sqrt{\frac{r-1}{2\pi K}} \exp\left[-K\left(1 - \frac{\log r}{r-1}\right)\right]. \quad (34)$$

Fig. 2 also shows f_j^* as a function of j for six stable steady states corresponding to different values of m and K . Results similar to those shown in the six panels on the rhs of Fig. 2 are given in Fig. 2 in (Nachman, 2000), and in Fig. 2 **a-c** in (Casagrandi and Gatto, 2002).

One observes how the number of empty patches f_0^* tends towards unity as the critical line is approached. To leading order in δ we have:

$$f_0^* = 1 - c_1\delta. \quad (35)$$

The constant c_1 is given in appendix B. Similarly, the expected number of individuals per patch approaches zero:

$$\sum_{j=1}^{\infty} j f_j^* \sim c_2 \delta \quad (36)$$

as $\delta \rightarrow 0$. The constant c_2 is given in appendix B. Fig. 3 shows the average number of individuals per patch, and $1 - f_0^*$ as a function of m . Shown are numerical solutions of the steady-state condition (30), solid lines, of Eqs. (35) and (36), dashed lines, and of direct numerical simulations (symbols) of the metapopulation model described in section 2.2. The numerical experiments were performed for $N = 50, 100$ and 1000 patches and averaged over an ensemble of different realisations. In principle, in a finite metapopulation no stable steady states exist with $f_j^* > 0$ for some $j \geq 1$. But the larger the number of patches, the larger the average time to extinction is expected to be. $N = 1000$, it turns out, is sufficiently large for the parameter values chosen that extinction did not occur during the simulations. Consequently we observe good agreement between the direct numerical simulations and the numerical solution of the deterministic steady-state condition. When the number of patches is small, by contrast, this is no longer the case, and it becomes necessary to estimate the time to extinction (see section 3.2.3). In order to determine the quasi-steady state in such cases, the simulations must be run for a time large enough for the initial transient to die out, but shorter than the expected time to extinction. Stochastic realisations leading to extinction during the simulation time must be discarded.

3.1.2. Relaxation dynamics in the limit of $N \rightarrow \infty$ and Levins' model

We continue to discuss metapopulations with infinitely many patches. In this section we analyse how the metapopulation relaxes to the stable steady state \mathbf{f}^* . This question is important for two reasons. First, when the relaxation time is much smaller than the expected time to extinction (that is when the number of patches is large enough), Eq. (15) describes the relaxation dynamics well. Second, and more importantly, the deterministic dynamics exhibits a ‘slow mode’ in the vicinity of the critical line (in Fig. 2): for small values of δ , it turns out, there is a particular linear combination of the variables f_j that relaxes slowly, with a rate proportional to δ . This slow mode dominates the relaxation dynamics which is thus essentially one-dimensional for small values of δ . This fact is well known in the theory of dynamical systems (Guckenheimer and Holmes, 1983), see also Dykman et al. (1994). For our model, this fact has important implications. Essentially, the deter-

ministic dynamics close to the critical line in Fig. 2 reduces to Levins' model, as we demonstrate in this section.

Fig. 4 shows the relaxation of the average number of individuals and of the frequency of empty patches f_0 to their values in the stable steady state \mathbf{f}^* , for three different initial conditions. Shown are numerical solutions of Eqs. (15,17), solid lines, as well as results of direct numerical simulations, symbols. The numerical experiments were performed for $N = 50, 100$ and 1000 patches, and averaged over 100 realisations. Even for 50 patches, and for the parameter values chosen in Fig. 4, the average time to extinction is large enough so that extinction did not occur in the numerical simulations. The agreement between the direct numerical simulations for $N = 1000$ and the solution of Eqs. (15,17) is good. For $N = 50$ and 100 we can observe deviations to the solution of Eqs. (15,17). Here the effect of the finite number N of patches becomes apparent.

In general Eqs. (15,17) must be solved numerically. We now show that the deterministic dynamics simplifies considerably close to the critical line in Fig. 2, when δ is small. At $\delta = 0$ we have that $I^* = 0$, $f_0^* = 1$ and consequently $\mathbf{f}^* = \mathbf{0}$. For small positive values of δ , the components of \mathbf{f}^* are of order δ , and we expand Eq. (15) in powers of δ and \mathbf{f} :

$$v_i = \sum_j A_{ij}^{(0)} f_j + m_c \delta \sum_j A_{ij}^{(1)} f_j + \frac{1}{2} m_c (1 + \delta) \sum_{jk} A_{ijk}^{(2)} f_j f_k. \quad (37)$$

Here $A_{ij}^{(0)}$ are the elements of the matrix \mathbf{A} evaluated at the critical line ($\delta = 0$). They are obtained from (A.2):

$$\begin{aligned} A_{ij}^{(0)} &= b_{i-1} \delta_{i-1,j} + (d_{i+1} + m_c(i+1)) \delta_{i+1,j} - (b_i + d_i + m_c i) \delta_{ij} \quad \text{for } i > 1, \\ A_{1j}^{(0)} &= (d_2 + 2m_c) \delta_{j2} - (b_1 + d_1 + m_c) \delta_{j1} + m_c j. \end{aligned} \quad (38)$$

The slow mode exists because this matrix has one zero eigenvalue, λ_1 (all other eigenvalues are negative). At finite but small values of δ the corresponding matrix (A.2) evaluated at the steady state \mathbf{f}^* has one small eigenvalue, $\lambda_1 \sim -\delta$, as shown in Fig. 5. To identify the slow mode we diagonalise $\mathbf{A}^{(0)}$ given by (38). Since this matrix is not symmetric, its left and right eigenvectors differ:

$$\mathbf{A}^{(0)} |R_\alpha\rangle = \lambda_\alpha |R_\alpha\rangle, \quad \langle L_\beta | \mathbf{A}^{(0)} = \langle L_\beta | \lambda_\beta, \quad \text{for } \alpha = 1, 2, \dots \quad (39)$$

Here $|f\rangle$ represents the vector \mathbf{f} , and $\langle f|$ represents its transpose. We take the eigenvectors to be bi-orthogonal, $\langle L_\beta | R_\alpha\rangle = \delta_{\alpha\beta}$. As before, the eigenvalues are

ordered as $0 \geq \lambda_1 > \lambda_2 > \dots$. Multiplying (37) from the left with $\langle L_\alpha |$ and making use of (15) yields an equation of motion for $Q_\alpha = \langle L_\alpha | f \rangle$:

$$\begin{aligned} \frac{dQ_\alpha}{dt} &= \langle L_\alpha | \mathbf{A}^{(0)} | f \rangle + m_c \delta \sum_{ij\beta} L_{\alpha i} A_{ij}^{(1)} R_{\beta j} Q_\beta \\ &\quad + \frac{1}{2} m_c (1 + \delta) \sum_{ijk\mu\nu} L_{\alpha i} A_{ijk}^{(2)} R_{\mu j} R_{\nu k} Q_\mu Q_\nu. \end{aligned} \quad (40)$$

At $m = m_c$ (that is for $\delta = 0$) we have that $\lambda_1 = 0$. For small values of δ we find $|\lambda_1| \ll |\lambda_\alpha|$ for $\alpha > 1$. This is apparent from Fig. 5. While λ_α , $\alpha > 1$, approach constants as $\delta \rightarrow 0$, $\lambda_1 = \langle L_1 | \mathbf{A}^{(0)} | R_1 \rangle \propto -\delta$ tends to zero in this limit. We thus expect that

$$\left| \frac{dQ_1}{dt} \right| \ll \left| \frac{dQ_\alpha}{dt} \right| \quad \text{for } \alpha > 1. \quad (41)$$

In the following, Q_1 is therefore referred to as ‘slow mode’, whereas Q_α for $\alpha > 1$ are termed fast variables. The fast variables rapidly approach quasi-steady states

$$Q_\alpha \approx -\frac{a_{\alpha 1} \delta Q_1 + a_{\alpha 2} Q_1^2}{\lambda_\alpha} \quad \text{for } \alpha > 1 \quad (42)$$

that depend on the instantaneous value of the slow variable, Q_1 . Terms including fast variables (Q_α for $\alpha > 1$) are not kept on the right-hand side of (42) because they are of higher order in δ . This is a consequence of the fact that close to the steady state, Q_1 is of order δ . Eq. (42) is correct to order δ^2 . The coefficients $a_{\alpha 1}$ and $a_{\alpha 2}$ are given by

$$\begin{aligned} a_{\alpha 1} &= m_c \sum_{ij} L_{\alpha i} A_{ij}^{(1)} R_{1j}, \\ a_{\alpha 2} &= \frac{m_c}{2} \sum_{ijk} L_{\alpha i} A_{ijk}^{(2)} R_{1j} R_{1k}, \end{aligned} \quad (43)$$

for $\alpha = 1, 2, \dots$. The elements $A_{ij}^{(1)}$ and $A_{ijk}^{(2)}$ are given in appendix A. The equation of motion for the slow mode Q_1 is to third order in δ :

$$\begin{aligned} \frac{dQ_1}{dt} &= a_{11} \delta Q_1 + a_{12} (1 + \delta) Q_1^2 \\ &\quad + \text{terms of order } \delta^3 \text{ involving } Q_\beta \text{ for } \beta > 1 \\ &\quad + \text{terms of higher order in } \delta. \end{aligned} \quad (44)$$

In the remainder of this subsection we neglect the δ^3 -terms and higher-order terms in (44). The δ^3 -terms are discussed in subsection 3.2. To second order in δ , the equation of motion for Q_1 is:

$$\frac{dQ_1}{dt} = a_{11}\delta Q_1 + a_{12}Q_1^2. \quad (45)$$

According to (43), the coefficients a_{11} and a_{12} are given in terms of the components L_{1j} of the left eigenvector $\langle L_1|$ and the components R_{1j} of the right eigenvector $|R_1\rangle$ of $\mathbf{A}^{(0)}$. For the right eigenvector we find, from Eqs. (38) and (39),

$$R_{1j} = R_{11} \prod_{k=2}^j \frac{b_{k-1}}{d_k + m_c k} \quad \text{for } j > 1, \quad \text{the first component being } R_{11}. \quad (46)$$

For the left eigenvector, we obtain the following recursion (with the boundary condition $L_{1j} = 0$ for $j = -1$):

$$L_{1j+1} - L_{1j} = \frac{d_j + m_c j}{b_j} (L_{1j} - L_{1j-1}) - \frac{m_c j}{b_j} L_{11}. \quad (47)$$

This recursion is solved by:

$$\begin{aligned} L_{11}, \quad L_{12} &= L_{11} \left(1 + \frac{d_1}{b_1} \right), \quad \text{and} \\ L_{1j} &= L_{11} \left(1 + \frac{d_1}{b_1} + \frac{m_c}{b_1} \sum_{n=2}^{j-1} \sum_{k=n+1}^{\infty} \frac{k R_{1k}}{n R_{1n}} \right) \quad \text{for } j > 2. \end{aligned} \quad (48)$$

We show in appendix C that the elements of $\langle L_1|$ approach the following limiting form as $K \rightarrow \infty$:

$$L_{11}, \quad L_{12} = L_{11} \frac{r+1}{r}, \quad \text{and} \quad L_{1j} = L_{11} r \frac{1-r^{-j}}{r-1}. \quad (49)$$

We choose L_{11} such that L_{1j} approaches unity for $j \gg 1$ as $K \rightarrow \infty$. This corresponds to the choice $L_{11} = (r-1)/r$, resulting in

$$L_{1j} = 1 - r^{-j} \quad (50)$$

in the limit of $K \rightarrow \infty$. In this limit, and for large values of r , we see that $\langle L_1|$ approaches the vector $(1, 1, \dots)$. The convention leading to (50) also fixes R_{11}

which must be chosen so that $\langle L_1 | R_1 \rangle = 1$. Explicit expressions for a_{11} and a_{12} , obtained from (43), (46), and (48) are given in appendix B.

Eq. (45) has two steady states $Q_1 = 0$ and $Q_1^* = -a_{11}\delta/a_{12}$. Note that Q_1^* is positive since $a_{12} < 0$. These two steady states correspond to the steady states $f = 0$ and f^* of (15). Comparison with (29) shows that $|R_1\rangle$ is proportional to $|f^*\rangle$ to lowest order in I^* (that is to lowest order in δ). In fact we have

$$|f^*\rangle = |R_1\rangle Q_1^* + \text{higher orders in } \delta. \quad (51)$$

Fig. 6 shows a comparison between $|f^*\rangle$ and $|R_1\rangle Q_1^*$ for $\delta = 0.1$. We see that this value of δ is small enough for (51) to work well.

Fig. 7 illustrates how the deterministic dynamics relaxes to the stable steady state f^* . Shown are the expected number of individuals per patch, $\sum_j j f_j$ and the number of empty patches as functions of time, determined from numerical solutions of (15,17). Curves for three different initial conditions are shown (solid lines), both on a linear time scale (top) as well as on a logarithmic time scale (bottom). The corresponding solutions of (45) are shown as dashed lines. Initially the variable Q_1 is not much slower than the Q_α -variables for $\alpha > 1$, and the approximate one-dimensional dynamics (45) is not a good approximation. But the solution of Eqs. (15,17) rapidly relaxes to a form where Q_1 becomes a slow mode, and (45) accurately describes the slow approach to the steady state.

Comparing Eqs. (45) and (1) shows that the slow mode Q_1 obeys Levins' equation. The results of this subsection allow us to compute e and c in terms of r , K , and δ . We find to order δ

$$\begin{aligned} c - e &= a_{11}\delta, \\ c &= -a_{12} + \text{terms of order } \delta. \end{aligned} \quad (52)$$

The contributions to c of order δ can be computed explicitly using the formulae derived above. For the sake of brevity we do not specify these contributions here. In Sec. 3.2.3 we give an explicit formula valid in the limit of large K .

We see that that Levins' model describes the dynamics of the metapopulation regardless of whether the patches are strongly coupled or not, provided the metapopulation is sufficiently close to criticality (that is close to the red line in Fig. 2). But we emphasise that in general the slow variable is not the fraction of occupied patches as envisaged by Levins. The variable Q_1 is given by $\langle L_1 | f \rangle$. Fig. 8 shows how the components L_{1j} of $\langle L_1 |$ depend upon j . When the local population dynamics is fast compared to the migration dynamics (for $r = 1.5$ and $K = 50$), the vector is approximately given by $(1, 1, 1, \dots)$, see also (50). In

this case, Q_1 is approximately equal to the fraction Q of occupied patches. This is the limit of time-scale separation considered by Levins. We have thus been able to derive the coefficients appearing in (1) from a stochastic, individual-based metapopulation model defined in terms of local birth and death rates, as well as the migration rate. Fig. 9 shows the dependence of a_{11} and a_{12} on K for $r = 1.05$ and $r = 1.5$, along with their asymptotic behaviours for large values of K . The latter is given by (see appendix C):

$$a_{11} \sim -a_{12} \sim \sqrt{\frac{K(r-1)^3}{2\pi}} \exp\left[-K\left(1 - \frac{\log r}{r-1}\right)\right]. \quad (53)$$

When the patches are strongly mixed by migration, then the interpretation of Q_1 is different. Fig. 8 shows that for $r = 1.05$ and $K = 10$, the components L_{1j} are roughly proportional to j in the relevant range of j (where f_j^* is not too small). In this case, therefore, the slow mode is interpreted as the average number of individuals per patch, which in turn is proportional to the immigration rate (10).

In summary, in this section we have shown how the deterministic metapopulation dynamics simplifies in the vicinity of the bifurcation (red line in Fig. 2), that is, for small values of δ . In this limit, the deterministic dynamics is essentially one-dimensional, and of the same form as the deterministic equation for the fraction of occupied patches originally suggested by Levins (1969). Commonly it is argued that the form (1) is appropriate when the local dynamics is much faster than migration. We have seen that this is not a necessary condition. In general, Eq. (1) describes the deterministic dynamics of metapopulations on the brink of extinction (for small values of δ). We find that the variable Q is indeed given by the fraction of occupied patches when the local-patch dynamics is fast. In general, however, Q has a different interpretation. Last but not least, we have been able to relate the effective rates c and e to the parameters of the individual-based, stochastic model (namely r , K , and $\delta = (m - m_c)/m_c$).

3.2. Finite number of patches

In the previous section we summarised our results on metapopulation dynamics in the limit of $N \rightarrow \infty$. The subject of the present section is the dynamics for metapopulations consisting of a finite number N of patches. In this case the fluctuations inherent in the birth-, death- and migration processes lead to fluctuations around the steady state \mathbf{f}^* . When the number of patches is large, these fluctuations are expected to be small. But they are essential: in a finite metapopulation the only absorbing state is $\mathbf{f} = \mathbf{0}$. In other words, the fluctuations turn the stable steady state \mathbf{f}^* of the deterministic dynamics into an unstable one.

3.2.1. Fluctuations around the quasi-steady state

For finite values of N , the population fluctuates around its quasi-steady state, as pointed out in section 2.4.2. These fluctuations are Gaussian and of order N^{-1} as Eqs. (18) and (26) show, and can be calculated by computing \mathbf{C} from (28). Fig. 10 (left) shows the N -dependence of the standard deviation of the fraction of empty patches σ_0 , which can be calculated from \mathbf{C} as

$$\sigma_0^2 = \langle f_0^2 \rangle - \langle f_0 \rangle^2 = \frac{1}{N} \sum_{i,j=1}^{\infty} C_{ij}. \quad (54)$$

Fig. 10 (right) shows the variance for each $\sigma_j^2 = \langle f_j^2 \rangle - \langle f_j \rangle^2$ as a function of j . We see that the agreement with direct simulations is good, for N of the order of 100.

3.2.2. Most likely path to extinction at finite but large values of N

When the number of patches is large, the state \mathbf{f}^* may be very long-lived (and is thus referred to as a quasi-steady state). The methods described in section 2.4 allow us to systematically analyse the properties of this quasi-steady state in terms of the auxiliary dynamics (21): while the deterministic dynamics in the limit of $N \rightarrow \infty$ is given by the deterministic Eq. (15), the stochastic dynamics of finite (but large) metapopulations is described by the auxiliary dynamics (21). We note that by setting $\mathbf{p} = \mathbf{0}$ in the auxiliary equations of motion (21), the deterministic dynamics (15) is obtained. In order to describe the fluctuations of a finite metapopulation around \mathbf{f}^* we need to find the optimal path from \mathbf{f}^* to a point \mathbf{f} in the vicinity, namely the path from \mathbf{f}^* to \mathbf{f} with extremal action (23), satisfying $H(\mathbf{f}(t), \mathbf{p}(t)) = 0$, as well as the boundary condition (27).

The tails of the quasi-steady state distribution near $\mathbf{f} = \mathbf{0}$ are obtained by computing the extremal path from \mathbf{f}^* to $\mathbf{f} = \mathbf{0}$. This path is termed the most likely path to extinction, because in the limit of large values of N the trajectories of the stochastic, individual-based dynamics to extinction are expected to fluctuate tightly around this path. The most likely path to extinction leaves the saddle point $(\mathbf{f}^*, \mathbf{0})$ along an unstable direction. Therefore this path cannot directly connect to the origin $(\mathbf{0}, \mathbf{0})$. It turns out that the auxiliary dynamics exhibits a saddle point at $\mathbf{f} = \mathbf{0}$ and at non-vanishing momenta, which we call \mathbf{p}^* . The steady-state condition $d\mathbf{p}/dt = \mathbf{0}$ gives rise to a recursion relation for the momentum components of \mathbf{p}^* of this saddle point:

$$e^{p_{k+1}^* - p_k^*} - 1 = \frac{d_k}{b_k} (1 - e^{-p_k^* + p_{k-1}^*}) + \frac{m_k}{b_k} (1 - e^{p_1^* - p_k^* + p_{k-1}^*}). \quad (55)$$

The problem lies in finding the optimal path from $(\mathbf{f}^*, \mathbf{0})$ to $(\mathbf{0}, \mathbf{p}^*)$. The manifold connecting these two points is infinite dimensional. It is straightforward to truncate the auxiliary system of equations at some large value of j , but finding the extremal path in the high-dimensional manifold (for instance by a numerical shooting method starting in the vicinity of \mathbf{f}^*) is very difficult.

However, the problem simplifies considerably in vicinity of the red line in Fig. 2. When δ is small, the auxiliary dynamics (21) is approximately two-dimensional, since the linearisation (25) has two small eigenvalues when $\delta \ll 1$. We write

$$\begin{aligned} \mathbf{J}|\mathcal{R}_\alpha\rangle &= \lambda_\alpha|\mathcal{R}_\alpha\rangle, \\ \mathbf{J}|\mathcal{R}'_\alpha\rangle &= -\lambda_\alpha|\mathcal{R}'_\alpha\rangle, \end{aligned} \quad (56)$$

and corresponding equations for the left eigenvectors $\langle\mathcal{L}_\alpha|$ and $\langle\mathcal{L}'_\alpha|$. Here λ_α are the eigenvalues of $\mathbf{A}^{(0)}$. The left and right eigenvectors of \mathbf{J} can be written in terms of those of $\mathbf{A}^{(0)}$:

$$|\mathcal{R}'_\alpha\rangle = \begin{pmatrix} \mathbf{C}|\mathcal{L}_\alpha\rangle \\ |\mathcal{L}_\alpha\rangle \end{pmatrix}, \quad \text{and} \quad |\mathcal{R}_\alpha\rangle = \begin{pmatrix} |\mathcal{R}_\alpha\rangle \\ 0 \end{pmatrix}. \quad (57)$$

The left eigenvectors are given by

$$\langle\mathcal{L}'_\alpha| = (0, \langle\mathcal{R}_\alpha|), \quad \text{and} \quad \langle\mathcal{L}_\alpha| = (\langle\mathcal{L}_\alpha|, -\langle\mathcal{L}_\alpha|\mathbf{C}). \quad (58)$$

Here \mathbf{C} is the covariance matrix (multiplied by N) of the Gaussian distribution of $\delta\mathbf{f} = \mathbf{f} - \mathbf{f}^*$ around \mathbf{f}^* , see (26).

The slow variables are obtained by projecting $(\mathbf{f}, \mathbf{p})^\top$ onto $\langle\mathcal{L}_1|$ and $\langle\mathcal{L}'_1|$ at $\delta = 0$. Since $\mathbf{C} = 0$ for $\delta = 0$, the slow variables are simply Q_1 and P_1 , where

$$Q_\alpha = \langle\mathcal{L}_\alpha|\mathbf{f}\rangle \quad \text{and} \quad P_\alpha = \langle\mathcal{L}'_\alpha|\mathbf{p}\rangle. \quad (59)$$

The slow dynamics of Q_1 and P_1 is found by expanding the Hamiltonian (20) in powers of δ , \mathbf{f} , and \mathbf{p} . Starting from (24), we use (37), as well as the expansion of $\mathbf{D}(\mathbf{f})$ in powers of \mathbf{f} . Noting that \mathbf{D} vanishes at criticality, we write

$$D_{ij} = \sum_{k=1}^{\infty} B_{ijk}^{(1)} f_k + \dots \quad (60)$$

The elements of $B_{ijk}^{(1)} = \partial D_{ij} / \partial f_k$ are given in appendix A. $H(Q_1, P_1)$ has the form (to third order in δ)

$$H(Q_1, P_1) = P_1(a_{11}\delta Q_1 + a_{12}Q_1^2) + b_{11}Q_1P_1^2. \quad (61)$$

The coefficients

$$b_{11} = \frac{1}{2} \sum_{ijk} L_{1i} B_{ijk}^{(1)} L_{1j} R_{1k}. \quad (62)$$

and a_{11}, a_{12} are given in appendix B. The equation of motion for Q_1 and P_1 is

$$\frac{dQ_1}{dt} = \frac{\partial H}{\partial P_1} \quad \text{and} \quad \frac{dP_1}{dt} = -\frac{\partial H}{\partial Q_1}. \quad (63)$$

The auxiliary dynamics determined by (61,63) has three steady states of interest for the questions addressed here:

$$Q_1 = 0 \quad \text{and} \quad P_1 = 0, \quad (64)$$

$$Q_1 = 0 \quad \text{and} \quad P = P_1^* = -a_{11}\delta/b_{11}, \quad (65)$$

$$Q_1 = Q_1^* = -a_{11}\delta/a_{12} \quad \text{and} \quad P_1 = 0. \quad (66)$$

All three steady states are saddle points. The steady state (66) corresponds to the saddle point $(f^*, \mathbf{0})$ of the full auxiliary dynamics (21). Note that $a_{12} < 0$. The steady state (65) corresponds to the saddle point $(\mathbf{0}, p^*)$ which lies at the end of the most likely path to extinction. In one-dimensional single-step birth-death processes, the corresponding point is commonly referred to as ‘fluctuational extinction point’. To lowest order in δ we have

$$\langle p^* | = P_1^* \langle L_1 | \quad + \quad \text{higher orders in } \delta. \quad (67)$$

Eq. (67) furnishes an interpretation of the left eigenvector $\langle L_1 |$ for small values of δ . This vector is proportional to the vector p^* , and the components of this vector define the coordinates of the fluctuational extinction point. In one-dimensional birth-death processes, the corresponding value is given by $p^* = -\log R_0$ where R_0 is the reproductive value. An example is the so-called SIS-model (Doering et al., 2005; Assaf and Meerson, 2010), a stochastic model for the duration of the epidemic state of an infectious disease. Here the reproductive value R_0 is the expected number of infections caused, during its lifetime, by one infected individual introduced into a susceptible population. In infinite populations the epidemic persists provided $R_0 > 1$. This criterion is precisely analogous to the persistence criteria discussed in Sec. 2.4.2. When R_0 is only slightly larger than unity, $R_0 = 1 + \epsilon$, say, then $p^* \approx -\epsilon$.

In our case, the vector $\langle L_1 |$ plays the role of a reproductive *vector* (Fisher, 1930; Samuelson, 1977). Expanding the solution of the linearised deterministic

dynamics (15) in terms of the eigenvectors of $\mathbf{A}^{(0)}$ yields

$$|\delta f(t)\rangle = \sum_{\alpha=1}^{\infty} e^{\lambda_{\alpha} t} |R_{\alpha}\rangle \langle L_{\alpha}| \delta f(0)\rangle \sim e^{\lambda_1 t} |R_1\rangle \langle L_1| \delta f(0)\rangle \quad \text{at large times.} \quad (68)$$

We see that the components L_{1j} of the vector $\langle L_1|$ determine how much fluctuations of the number of patches with j individuals contribute to the relaxation towards the steady state in infinite metapopulations. In other words, the components of $\langle L_1|$ determine the susceptibility of patches with j individuals to stochastic fluctuations. We shall see below that this susceptibility determines the average time to extinction. We note that the correspondence (67) implies that the solution of the recursion (55) for p_j^* must be equivalent, to lowest order in δ , to the recursion (47) for the components of $\langle L_1|$, up to a factor. This is indeed the case. In analogy with the SIS-model discussed above, the coordinates of the vector $\langle L_1|$ parameterise the fluctuational extinction point.

Finally we note that the components of $\langle L_1|$ have a simple interpretation in the limit of $K \rightarrow \infty$. Comparing Eqs. (50) and (C.18) we see that the component L_{1j} is given by the probability of a single, isolated patch with j individuals to eventually reach its carrying capacity, K . This observation concludes our discussion of the nature of the fluctuational extinction point of the auxiliary dynamics (63).

The most likely escape path leads from the saddle (66) to the fluctuation extinction point (65). The path is parameterised by Q_1 and P_1 . Solving $H = 0$ for P_1 we find from (61) (discarding the trivial solution $Q_1 = P_1 = 0$)

$$P_1 = -b_{11}^{-1}(a_{11}\delta + a_{12}Q_1). \quad (69)$$

Eq. (69) together with Eqs. (51) and (67) imply that the \mathbf{f} - and \mathbf{p} -spectra move rigidly towards extinction. In other words, our analysis shows that on the path to extinction, both $\mathbf{f}(t)$ and $\mathbf{p}(t)$ retain their shape (initially given by the right and left eigenvectors $|R_1\rangle$ and $\langle L_1|$ of $\mathbf{A}^{(0)}$) to lowest order in δ .

In the limit of large carrying capacities (where the critical migration rate is small) one might expect that patches become extinct independently of each other. In this limit, the rate of extinction of single patches in the population is small, and the \mathbf{f} -spectrum relaxes rapidly to its rigid shape once a given patch has gone extinct. It is important to emphasise that the patches are nevertheless coupled by migration which gives rise, in this limit, to a small rate of colonisation of empty patches. Thus the average time T_{ext} to extinction for the whole system is not determined by the largest time of extinction of the N single patches (we discuss the time T_{ext} in the following subsection).

When the population is strongly mixed by migration, on the other hand, it is surprising that the \mathbf{f} - and \mathbf{p} -spectra move rigidly to extinction. Migration upholds a balance that causes the shape of the \mathbf{f} -spectrum to remain unchanged as the metapopulation comes closer to extinction. In other words, just the normalisation $1 - f_0$ changes.

We have attempted to verify the predictions of this subsection by direct numerical simulations of the stochastic, individual-based model. The result is shown in Fig. 11. The simulations were performed as follows. For 10,000 independent realisations we followed the metapopulation to extinction. For each realisation we analysed the path to extinction by tracing the stochastic trajectory back in time, starting at the time of extinction. We traced the trajectories back for the average time it takes to reach, using this procedure, the number of individuals that corresponds to the quasi-steady state. At each time point, the number of individuals per patch, and the fraction of occupied patches was computed. Fig. 11 shows the probability of observing a given number of individuals on occupied patches, conditional on the fraction of occupied patches, $1 - f_0$. The probability is colour coded: white corresponds to high probability, black to low probability. The left panel of Fig. 11 is consistent with the prediction that the \mathbf{f} -spectrum moves rigidly. This is not the case for the case shown in the right panel of Fig. 11. Here δ is too large, the two-dimensional approximation to the auxiliary dynamics (21) is not accurate.

An alternative representation of the path to extinction is depicted in Fig. 12. Employing the same simulations described above, Fig. 12 shows the average n_j -spectrum conditional on the total number of individuals, compared with the trajectory obtained by numerically integrating the full auxiliary dynamics (21). We observe that the agreement is good up to a point where n_j becomes too small. When the total number of individuals is small (less than 30 for the parameters in Fig. 12) discrete effects start to dominate, and the large- N expansion of the Master equation fails to accurately describe the last part of the trajectory towards extinction.

3.2.3. Time to extinction for finite but large values of N

The tail of the quasi-steady state distribution (18) towards $\mathbf{f} = \mathbf{0}$ determines the average time to extinction. It is expected (Dykman et al., 1994) to scale as

$$T_{\text{ext}} = A \exp(NS). \quad (70)$$

The coefficient A may depend on N , as well as on r , K , and m . We have not been able to determine it. The action $S \equiv S(\mathbf{0})$ is a function r , K , and m . Since NS

appears in the argument of the exponential in (70), the average time to extinction depends sensitively upon the number N of patches, and on S (which in turn depends upon r , K , and m). Close to the critical line in Fig. 2 we find the action by integrating P_1 along the path (69). This gives:

$$S = -\frac{\delta^2}{2} \frac{a_{11}^2}{b_{11}a_{12}} \quad (71)$$

(note that $a_{12} < 0$). This prediction is compared to results of direct simulations in Figs. 13 to 15. The initial condition for the direct simulations was chosen as follows. First \mathbf{f}^* was calculated, this determines the initial state $\mathbf{n} = N\mathbf{f}^*$. Note however that the components n_j of \mathbf{n} must be integers. For small values of δ , all $n_{j>0}$ may round to zero, inconsistent with the constraint $\sum_j n_j = N$. In such cases we grouped counts n_j corresponding to neighbouring values of j together before rounding. The action S was determined by plotting $\log T_{\text{ext}}$ as a function of N . For sufficiently large values of N (such that $NS \gg 1$) one expects a straight line. We perform a linear regression by least squares to determine the slope S/δ^2 . Figs. 13 to 15 show $\log T_{\text{ext}}$ as a function of $N\delta^2$. The approximations leading to (71) require that N is large and δ small. Eq. (70) is expected to be a good approximation provided

$$(NS)^{-1/2} \ll \delta \ll 1. \quad (72)$$

The data shown in Figs. 13 to 15 are consistent with this expectation. We see that the fitted values of S approach the analytical result (71) as δ is decreased, right panels in Figs. 13 to 15. These figures illustrate the sensitive dependence of the time to extinction upon r , K , δ , and N .

In Fig. 16 we summarise our best estimates for S/δ^2 for different values of r and K (and for the smallest value of δ for which we obtained reliable results). These estimates are compared to the analytical result (71). We observe good agreement. Fig. 16 appears to indicate that S/δ^2 approaches the value $1/2$ as K increases. The approach appears to be the faster the larger the value of r is. In order to demonstrate that this is in fact true, we have determined the asymptotic dependency of the coefficient b_{11} upon K in the limit of large values of K . We find (see appendix C):

$$b_{11} \sim \sqrt{\frac{K(r-1)^3}{2\pi}} \exp\left[-K\left(1 - \frac{\log r}{r-1}\right)\right]. \quad (73)$$

This result, taken together with (53) determines the limiting value of S/δ^2 to be $1/2$. Fig. 16 shows that already for $r = 1.5$ and $K = 25$ the value of S/δ^2 is

very close to the limiting value. We note that while the expressions (53) and (73) depend upon K , the action (71) approaches a limit independent of K for large values of K . In this limit, the metapopulation dynamics can be understood in terms of a stochastic dynamics of the fraction of occupied patches.

Such an approach was suggested by Lande et al. (1998). In the following we briefly describe the similarities and differences between our asymptotic result, and the approach suggested by Lande et al. (1998). As already pointed out in the introduction, their analysis rests on four main assumptions: First, Lande et al. (1998) consider the limit of fast local dynamics and slow migration (time-scale separation). In our model, this corresponds to the limit $K \rightarrow \infty$ and to large values of r . Second, Lande et al. (1998) argue that the extinction rate in the stochastic model for the evolution of the number of occupied patches is given by the inverse time to extinction of a single patch, initially at carrying capacity. Third it is assumed that the rate of successful colonisation is given by the product of the expected number of migrants and the probability that an empty patch invaded by one migrant grows to its (quasi-)steady state. Fourth, Lande et al. (1998) allow for the possibility that the number of individuals per patch on occupied patches changes as the metapopulation approaches extinction, and argue that this effect can be incorporated in terms of effective rates $c(Q)$ and $e(Q)$.

Here we have shown, however, that in the limit of small values of δ the dynamics of f on the most likely path to extinction is rigid: f does not change its shape, just its normalisation. This implies, in particular, that the average number of individuals on occupied patches must remain unchanged as extinction is approached. This is clearly seen in Fig. 11 (left panel). We note, however, that the right panel of Fig. 11 shows that for larger values of δ , f does change its shape (and the average number of individuals on occupied patches decreases as extinction is approached). A first-principles theory for this effect is lacking. We refer to this point in the conclusions.

Let us now consider the parameterisations of the rates e and c suggested by Lande et al. (1998), Eqs. (3) and (4) in their paper. We have obtained analytical results in the vicinity of the bifurcation (that is, for small values of δ). In order to compare our results to the choices adopted by Lande et al. (1998) we must take the limit $K \rightarrow \infty$. In this limit, it turns out, that the terms of order δ^3 (and higher) in the second and third rows of Eq. (44) are negligible compared to the terms in the first row. In the limit of large values of K we can therefore conclude:

$$c = -(1 + \delta)a_{12} \quad \text{and} \quad e = c - a_{11}\delta. \quad (74)$$

The asymptotic expressions for a_{11} and a_{12} are given in Eq. (53). In appendix

C we have shown that these relations correspond precisely to the asymptotic K -dependence of the time T_K to extinction for a single isolated patch at carrying capacity. In the limit of large K (which is the limit Lande et al. (1998) consider) we thus have:

$$e = \frac{1}{T_K}. \quad (75)$$

This equation implies that the rate of extinction of patches in the coupled system does not depend upon δ to leading order in δ . In other words, patches go extinct independently in the limit $K \rightarrow \infty$. Eq. (75) closely resembles Eq. (4) in Lande et al. (1998).

Now consider the rate of successful colonisation. In the limit of $K \rightarrow \infty$, the probability of a single patch growing from one migrant to carrying capacity is $u_{1K} \sim (r - 1)/r$ (see appendix C). Immigration is irrelevant in this context since the local patch dynamics is assumed to be much faster than migration. Using this expression for u_{1K} and (34) for m_c we find the following expression for c

$$c = m_c(1 + \delta)Ku_{1K} = mKu_{1K}. \quad (76)$$

This result closely resembles Eq. (3) in Lande et al. (1998). We emphasise that our results are exact in the limit of small values of δ and large values of N and K .

A further minor difference is that Lande et al. (1998) employ the diffusion approximation to evaluate (3) and (4). This approximation fails unless r is close to unity.

We conclude this section with a discussion of (71). Eqs. (51,67) allow us to express the average time to extinction in the following form:

$$\log T_{\text{ext}} \sim \frac{N}{2} \langle -p^* | f^* \rangle = \frac{N}{2} \sum_{j=1}^{\infty} (-p_j^*) f_j^*. \quad (77)$$

Here $|f^*\rangle$ is the quasi-steady state distribution, and the vector $\langle -p^*|$ determines the susceptibility of patches with j individuals to stochastic fluctuations of the number of individuals. As explained above, the components $-p_j^*$ are related to Fisher's reproductive vector characterising the susceptibility, for example, of age classes in matrix population models. But note that in our case the components of $\langle p^*|$ do not characterise the properties of classes of individuals, but of patches. In other words, (77) can be understood by viewing the metapopulation as a population of patches, or as a population of local populations, as originally envisaged by Levins (1969).

4. Conclusions

In this paper we have analysed metapopulation dynamics on the brink of extinction in terms of a stochastic, individual-based metapopulation model consisting of a finite number N of patches. The distance from the bifurcation point where infinitely large metapopulations cease to persist is parameterised by δ . In the limit of large (but finite) values of N and small values of δ we have been able to quantitatively describe the stochastic metapopulation dynamics. We have shown that metapopulation dynamics, for small values of δ , is described by a one-dimensional equation of the form of Levins' model, Eq. (1). In other words, we have achieved to derive this model, and to compute the parameters c and e in terms of the microscopic parameters describing the local population dynamics, and migration. We could show that Levins' model is valid independently of whether or not there is a time-scale separation between local and migration dynamics. The crucial condition is that the population is close to bifurcation. We note that in the absence of time-scale separation, the interpretation of the variable Q in Eq. (1) is no longer the fraction of occupied patches.

We could show that the deterministic limit of our model corresponds to metapopulation models discussed by Casagrandi and Gatto (2002) and Nachman (2000), who have studied the persistence of infinitely large metapopulations by analysing the stability of steady states. The corresponding persistence criteria (which we discuss in detail) do not allow to characterise the persistence of finite metapopulations. But the stochastic dynamics derived and analysed in this paper makes it possible to characterise the most likely path to extinction and to estimate the average time to extinction of the metapopulation. We have discussed differences and similarities between a particular asymptotic limit of our results, and the approach suggested by Lande et al. (1998). Fig. 17 summarises different limiting cases of our results, and connections to earlier studies.

While our approach results in a comprehensive description of metapopulation dynamics for the model we consider, many open questions remain. A technical point is that we have not yet been able to compute the prefactor A in the expression Eq. (70) for the average time to extinction. This is a difficult problem requiring matching the solutions found in this paper with corresponding solutions valid for small values n_j (the number of patches with j individuals). Such solutions are outside the scope of our large- N treatment.

As the title of our paper makes it clear, the results derived here are valid for metapopulations on the brink of extinction. Further work is required in order to understand the metapopulation dynamics further away from the red line in Fig. 2.

A number of important questions in metapopulation dynamics can be addressed with the approach described here. Consider for example the dynamics of structured metapopulations.

We plan to study core-satellite models (Hanski and Gyllenberg, 1993), where the metapopulation lives on two types of patches (large and small). Large patches have more persistent populations, while populations on smaller patches are relatively ephemeral. Thus, the large patches are, on average, sources and the small patches are sinks for the metapopulation as a whole. Another important question is the effect of environmental fluctuations. These can be modeled, for instance, by introducing a time-dependent contribution $\mu(t)$ to the death rate in Eq. (3). Taking this to be a random function of time makes it possible to employ the approach described by Schaper et al. (2012).

Last but not least, it is necessary to compare the predictions summarised here with those of models with an explicit space dependence. We expect that the predictions summarised here should be the more accurate the wider the spatial scale of migration is.

Acknowledgements. Financial support by Vetenskapsrådet, by the Centre for Theoretical Biology at the University of Gothenburg, and by the Göran Gustafsson stiftelse are gratefully acknowledged.

Appendix A Formulae for the matrix elements occuring in the expansion of the Master equation

The matrix $\mathbf{D}(\mathbf{f})$ has entries

$$\begin{aligned}
 D_{ij} = & \delta_{ij} \left((b_{i-1} + I)f_{i-1} + (d_{i+1} + m_{i+1})f_{i+1} + (b_i + I + d_i + m_i)f_i \right) \\
 & + \delta_{i+1j} \left(- (d_{i+1} + m_{i+1})f_{i+1} - (b_i + I)f_i \right) \\
 & + \delta_{i-1j} \left(- (b_{i-1} + I)f_{i-1} - (d_i + m_i)f_i \right) \\
 & + m_{i+1}f_{i+1}(f_{j-1} - f_j) + f_i(m_jf_j - m_{j+1}f_{j+1}) \\
 & + m_if_i(f_j - f_{j-1}) + f_{i-1}(m_{j+1}f_{j+1} - m_jf_j) \quad \text{for } i, j > 1,
 \end{aligned} \tag{A.1}$$

$$\begin{aligned}
 D_{1j} = & \delta_{j2} \left(- (d_2 + m_2)f_2 - (b_1 + I)f_1 \right) + m_2f_2(f_{j-1} - f_j) + m_1f_1(f_j - f_{j-1}) \\
 & + f_1(m_jf_j - m_{j+1}f_{j+1}) + \left(1 - \sum_{k=1}^{\infty} f_k \right) (m_{j+1}f_{j+1} - m_jf_j) \quad \text{for } j > 1,
 \end{aligned}$$

$$\begin{aligned}
 D_{i1} = & \delta_{i2} \left(- (d_2 + m_2)f_2 - (b_1 + I)f_1 \right) + m_2f_2(f_{i-1} - f_i) + m_1f_1(f_i - f_{i-1}) \\
 & + f_1(m_if_i - m_{i+1}f_{i+1}) + \left(1 - \sum_{k=1}^{\infty} f_k \right) (m_{i+1}f_{i+1} - m_if_i) \quad \text{for } i > 1,
 \end{aligned}$$

$$\begin{aligned}
 D_{11} = & I \left(1 - \sum_{k=1}^{\infty} f_k \right) + (d_2 + m_2)f_2 + (b_1 + I + d_1 + m_1)f_1 \\
 & + 2 \left(1 - \sum_{k=1}^{\infty} f_k - f_1 \right) (m_2f_2 - m_1f_1).
 \end{aligned}$$

The elements of \mathbf{A} are given by

$$\begin{aligned}
 A_{ij} = & (b_{i-1} + I)\delta_{i-1j} + (d_{i+1} + m_{i+1})\delta_{i+1j} - (b_i + I + d_i + m_i)\delta_{ij} \\
 & + m_j(f_{i-1} - f_i) \quad \text{for } i > 1,
 \end{aligned} \tag{A.2}$$

$$A_{1j} = (d_2 + m_2)\delta_{j2} - (b_1 + I + d_1 + m_1)\delta_{j1} - I + m_j \left(1 - \sum_{k=1}^{\infty} f_k - f_1 \right).$$

The elements of $\mathbf{A}^{(0)}$ are obtained by setting $\delta = 0$ in Eq. (A.2). The elements of $\mathbf{A}^{(1)}$ are found to be:

$$A_{ij}^{(1)} = \begin{cases} j(\delta_{i+1j} - \delta_{ij}) & \text{for } i > 1 \\ j(\delta_{j2} - \delta_{j1} + 1) & \text{for } i = 1 \end{cases}. \tag{A.3}$$

The matrix elements of $\mathbf{A}^{(2)}$ are given by:

$$A_{ijk}^{(2)} = \begin{cases} -k(\delta_{ij} - \delta_{i-1j}) - j(\delta_{ik} - \delta_{i-1k}) & \text{for } i > 1 \\ -k(\delta_{1j} + 1) - j(\delta_{1k} + 1) & \text{for } i = 1 \end{cases} \quad (\text{A.4})$$

The elements of $\mathbf{B}^{(1)}$ found to be:

$$\begin{aligned} B_{ijk}^{(1)} &= b_k[\delta_{ki-1}(\delta_{ij} - \delta_{ji-1}) + \delta_{ik}(\delta_{ij} - \delta_{ji+1})] \\ &\quad + (d_k + m_k)[\delta_{ki+1}(\delta_{ij} - \delta_{ji+1}) + \delta_{ik}(\delta_{ij} - \delta_{ji-1})] \quad \text{for } i, j > 1, \\ B_{1jk}^{(1)} &= (d_2 + m_2)(-\delta_{k2}\delta_{j2}) - b_1\delta_{k1}\delta_{j2} + m_k(\delta_{kj+1} - \delta_{kj}) \quad \text{for } j > 1, \\ B_{ilk}^{(1)} &= (d_2 + m_2)(-\delta_{k2}\delta_{i2}) - b_1\delta_{k1}\delta_{i2} + m_k(\delta_{ki+1} - \delta_{ki}) \quad \text{for } i > 1, \\ B_{11k}^{(1)} &= m_k + (d_2 + 3m_2)\delta_{k2} + (b_1 + d_1 - m_1)\delta_{k1}. \end{aligned} \quad (\text{A.5})$$

Appendix B Summary of results for coefficients used in section 3

In this appendix we give explicit expressions for the coefficients $I_1, c_1, c_2, a_{11}, a_{12}$ and b_{12} appearing in Eqs. (32), (35), (36), (45), and (61). First, the coefficient I_1 in Eq. (32) is calculated by expanding (30). Expanding to lowest order yields the condition (33) which gives m_c but does not determine I_1 . In order to find I_1 it is necessary to expand (30) to second order in δ . This requires expanding:

$$\begin{aligned} m_c(1 + \delta) \sum_{j=2}^{\infty} j \prod_{k=2}^j \frac{b_{k-1} + I^*}{d_k + m_c k} &= I_1 \delta - I_2 \delta^2 + g_1(I_1) \delta^2 + \dots, \\ \sum_{j=2}^{\infty} \prod_{k=2}^j \frac{b_{k-1} + I^*}{d_k + m_c k} &= g_0(I_1) \delta + \dots \end{aligned} \quad (\text{B.1})$$

We find:

$$g_0(I_1) = \frac{I_1}{d_1 + m_c} \left(1 + \sum_{j=2}^{\infty} \frac{R_{1j}}{R_{11}} \right) \quad (\text{B.2})$$

$$\begin{aligned} g_1(I_1) &= \frac{d_1}{d_1 + m_c} I_1 - \frac{m_c I_1}{d_1 + m_c} \sum_{k=2}^{\infty} \frac{k R_{1k}}{R_{11}} \sum_{i=2}^k \frac{m_c i}{d_i + m_c i} \\ &\quad + \frac{m_c I_1^2}{d_1 + m_c} \sum_{k=2}^{\infty} \frac{k R_{1k}}{R_{11}} \sum_{i=2}^k \frac{1}{b_{i-1}}. \end{aligned} \quad (\text{B.3})$$

Inserting these expansions into the self-consistency condition (30) gives:

$$I_1 = \frac{g_1(I_1)}{g_0(I_1)}. \quad (\text{B.4})$$

We find

$$I_1 = \frac{d_1 - m_c \sum_{k=2}^{\infty} \frac{k R_{1k}}{R_{11}} \sum_{i=2}^k \frac{m_c i}{d_i + m_c i}}{1 + \sum_{k=2}^{\infty} \frac{R_{1k}}{R_{11}} (1 - k \sum_{i=2}^k \frac{1}{b_{i-1}})}. \quad (\text{B.5})$$

Second, the coefficient c_1 determines the leading order of the δ -expansion of the fraction f_0^* of extinct patches in the steady state. To leading order in δ we have $f_0^*(\delta) \sim 1 - g_0(\delta)$. Thus the coefficient c_1 in (35) is given by

$$c_1 = \frac{I_1}{d_1 + m_c} \left(1 + \sum_{j=2}^{\infty} \frac{R_{1j}}{R_{11}} \right). \quad (\text{B.6})$$

Third, the coefficient c_2 determining the lowest order of an expansion of the number of individuals per patch (36) in powers of δ is given by the lowest-order term of (B.1). We find:

$$c_2 = \frac{I_1}{m_c}. \quad (\text{B.7})$$

Fourth, in order to find the coefficients a_{11} and a_{12} appearing in (45), we insert (A.4) and (A.3) into (43) for $\alpha = 1$. Using (46) and (48) yields

$$a_{11} = L_{11} R_{11} \left(d_1 - m_c \sum_{k=2}^{\infty} \frac{k R_{1k}}{R_{11}} \sum_{j=2}^k \frac{m_c j}{d_j + m_c j} \right), \quad (\text{B.8})$$

$$a_{12} = - (d_1 + m_c) L_{11} R_{11}^2 \left(1 + \sum_{k=2}^{\infty} \frac{R_{1k}}{R_{11}} \left(1 - k \sum_{j=2}^k \frac{m_c}{b_{j-1}} \right) \right). \quad (\text{B.9})$$

Finally, coefficient b_{11} in (61) is determined by inserting (A.1) into (62), which results in

$$b_{11} = \sum_{i=2}^{\infty} (d_i + m_c i) (L_{1i} - L_{1i-1})^2 R_{1i} - L_{11} \sum_{i=2}^{\infty} m_c i (L_{1i} - L_{1i-1}) R_{1i} + d_1 L_{11}^2 R_{11}. \quad (\text{B.10})$$

Appendix C Asymptotics for large values of K

In this appendix we briefly demonstrate how to obtain the asymptotics of the eigenvectors, of the coefficients a_{11} , a_{12} , b_{12} , and of the critical migration rate m_c

in the limit of $K \rightarrow \infty$ (see Eqs. (34) (53), and (73) in the main text). First, the results of this appendix demonstrate that the action (71) tends to $1/2$ as $K \rightarrow \infty$. Second, the results obtained below shed light on the connection of our results to the work of Lande et al. (1998).

In the limit of large carrying capacities K , the asymptotics of the coefficients a_{11}, a_{12}, b_{12} is given by the asymptotics of R_{11} which in turn is determined by the requirement that $\langle L_1 | R_1 \rangle = 1$. The first step consists of deriving the asymptotic form (34) of m_c in the limit of $K \rightarrow \infty$. The critical migration rate m_c is given by (33):

$$d_1 = m_c \sum_{j=2}^{\infty} j \prod_{k=2}^j \frac{b_{k-1}}{d_k + m_c k}. \quad (\text{C.1})$$

The product in this equation is estimated by exponentiation, taking the continuum limit, and the resulting integral is evaluated in the saddle-point approximation, exactly as described by Doering et al. (2005), see also (Mehlig and Wilkinson, 2007). Following Doering et al. (2005) we introduce the variable $x = i/K$ and define the functions $b(x)$ and $d(x)$ by

$$b_i = K b(x) \quad \text{and} \quad d_i = K d(x). \quad (\text{C.2})$$

In the limit of $K \rightarrow \infty$, the term $m_c k$ in the denominator in (C.1) is negligible compared to d_k . The product is then estimated using

$$\prod_{k=1}^{j-1} \frac{b_k}{d_k} \sim e^{K \int_0^y dx \log \rho(x) - \frac{1}{2}[(\log \rho(0) + \log \rho(y))]} = \frac{e^{-K\Phi(y)}}{\sqrt{\rho(0)\rho(y)}} \quad (\text{C.3})$$

with $y = j/K$, $\rho(x) = b(x)/d(x)$, and

$$\Phi(y) = - \int_0^y dx \log \rho(x) = - \int_0^y \frac{dx r}{1 + (r-1)x}. \quad (\text{C.4})$$

It follows that

$$\sum_{j=2}^{\infty} d_1 \frac{j}{d_j} \prod_{k=1}^{j-1} \frac{b_k}{d_k} \sim K^2 \int_0^{\infty} dy \frac{d_1}{d(y)} \frac{e^{-K\Phi(y)}}{\sqrt{\rho(0)\rho(y)}}. \quad (\text{C.5})$$

The integral is evaluated in the saddle-point approximation. The saddle point is $x_s = 1$. With $d^2\Phi/dx^2 = (r-1)/r$ at $x_s = 1$ we have:

$$\sum_{j=2}^{\infty} \frac{d_1}{d_j} \prod_{k=1}^{j-1} \frac{b_k}{d_k} \sim K^2 \sqrt{\frac{2\pi r}{K(r-1)}} \frac{1}{Kr} \frac{1}{\sqrt{r}} e^{\left[K \left(1 - \frac{\log r}{r-1} \right) \right]}, \quad (\text{C.6})$$

resulting in (34).

The second step consists of determining the limiting form (49) of the elements (48) of $\langle L_1 |$ in the limit of large values of K . We now show that the double sum in (48) grows exponentially, precisely cancelling the exponential decrease of m_c as $K \rightarrow \infty$. The calculation is very closely related to the evaluation of the time to extinction in a single-patch model analysed by Doering et al. (2005). We have

$$\sum_{n=2}^{j-1} \sum_{k=n+1}^{\infty} \frac{kR_{1k}}{nR_{1n}} \sim \frac{K^2}{Kr} \sqrt{\frac{2\pi r}{K(r-1)}} e^{\left[K\left(1-\frac{\log r}{r-1}\right)\right]} \sum_{n=2}^{j-1} \sqrt{\rho(0)} e^{-n \log r}. \quad (C.7)$$

Performing the geometric sum and inserting into (48) we obtain

$$L_{1j} = 1 - r^{-j}. \quad (C.8)$$

The third step consists of estimating R_{11} which is determined by the requirement

$$1 = \langle L_1 | R_1 \rangle \sim R_{11} \left(\frac{r-1}{r} + \sum_{j=2}^{\infty} (1-r^{-j}) \frac{d_1}{d_j} \prod_{k=1}^{j-1} \frac{b_k}{d_k} \right). \quad (C.9)$$

We proceed as before and obtain:

$$R_{11} \sim r \sqrt{\frac{K(r-1)}{2\pi}} e^{\left[-K\left(1-\frac{\log r}{r-1}\right)\right]}. \quad (C.10)$$

These results enable us to determine the coefficients a_{11} , a_{12} , b_{12} from Eqs. (B.8) to (B.10). In (B.8), the double sum is negligible compared to d_1 in the limit of $K \rightarrow \infty$. This implies

$$a_{11} \sim L_{11} R_{11} d_1 \sim \sqrt{\frac{K(r-1)^3}{2\pi}} e^{\left[-K\left(1-\frac{\log r}{r-1}\right)\right]}. \quad (C.11)$$

In (B.9), the sum over j is negligible compare to unity. Evaluating the sum over k in the asymptotic limit, we find:

$$a_{12} \sim -\sqrt{\frac{K(r-1)^3}{2\pi}} e^{\left[-K\left(1-\frac{\log r}{r-1}\right)\right]}. \quad (C.12)$$

Finally, (B.10) consists of three terms. The second term is negligible compared to the other two. We find:

$$b_{11} \sim \sqrt{\frac{K(r-1)^3}{2\pi}} e^{\left[-K\left(1-\frac{\log r}{r-1}\right)\right]}. \quad (C.13)$$

We see that the three coefficients have the same asymptotic dependence on K , apart from the minus sign in (C.12). It turns out that this asymptotic K -dependence is exactly the inverse of the asymptotic dependence of the time to extinction T_K for a single isolated patch with rates (2,3) upon K (no migration). The corresponding expression is given in (19) of Doering et al. (2005):

$$T_K = \sqrt{\frac{2\pi}{K(r-1)^3}} e^{\left[K \left(1 - \frac{\log r}{r-1} \right) \right]}. \quad (\text{C.14})$$

Last but not least let us consider the probability u_{1K} that a single isolated patch grows from one individual to its carrying capacity K . According to van Kampen (1981) one has:

$$u_{1K} = \left(1 + \sum_{i=1}^{K-1} \prod_{j=1}^i \frac{d_j}{b_j} \right)^{-1}. \quad (\text{C.15})$$

This expression becomes independent of K in the limit $K \rightarrow \infty$. Following the same procedure as above, we find in this limit:

$$u_{1K} \sim \frac{r-1}{r}. \quad (\text{C.16})$$

The corresponding probability to grow from j individuals to K is (van Kampen, 1981):

$$u_{jK} = \frac{1 + \sum_{i=1}^{j-1} \prod_{k=1}^i \frac{d_k}{b_k}}{1 + \sum_{i=1}^{K-1} \prod_{k=1}^i \frac{d_k}{b_k}}, \quad (\text{C.17})$$

This expression converges to

$$u_{jK} \sim 1 - r^{-j} \quad (\text{C.18})$$

as $K \rightarrow \infty$.

References

- Altland, A., Simons, B., 2010. Condensed Matter Field Theory, 2nd Edition. Cambridge University Press, Cambridge.
- Arrigoni, F., 2003. Deterministic approximation of a stochastic metapopulation model. Adv. Appl. Probab. 35, 691–720.

- Assaf, M., Meerson, B., 2010. Extinction of metastable stochastic populations. *Phys. Rev. E* 81, 021116.
- Casagrandi, R., Gatto, M., 1999. A mesoscale approach to extinction risk in fragmented habitats. *Nature* 400, 560–562.
- Casagrandi, R., Gatto, M., 2002. A persistence criterion for metapopulations. *Theor. Popul. Biol.* 61, 115–125.
- Chesson, P., 1984. Persistence of a markovian population in a patchy environment. *Z. Wahrscheinlichkeitstheor.* 66, 97–107.
- Chesson, P. L., 1981. Models for spatially distributed populations: The effect of within-patch variability. *Theor. Popul. Biol.* 19, 288–325.
- Doering, C. R., Sargsyan, K. V., Sander, L. M., 2005. Extinction times for birth-death processes: exact results, continuum asymptotics, and the failure of the Fokker–Planck approximation. *Multiscale Model. Simul.* 3, 283–299.
- Drechsler, M., Wissel, C., 1997. Separability of local and regional dynamics in metapopulations. *Theor. Popul. Biol.* 51, 9–21.
- Dykman, M. I., Mori, E., Ross, J., Hunt, P. M., 1994. Large fluctuations and optimal paths in chemical kinetics. *J. Chem. Phys.* 100, 5735–5750.
- Elgart, V., Kamenev, A., 2004. Rare event statistics in reaction-diffusion systems. *Phys. Rev. E* 70, 041106.
- Etienne, R., 2000. Local populations of different sizes, mechanistic rescue effect and patch preference in the levins metapopulation model. *B. Math. Biol.* 62, 943–958.
- Etienne, R., 2002. A scrutiny of the levins metapopulation model. *Comments Theor. Biol.* 7, 257–281.
- Fisher, R. A., 1930. *The genetical theory of natural selection*. Clarendon Press, Oxford.
- Freidlin, M. I., Wentzell, A. D., 1984. *Random Perturbations of Dynamical Systems*. Fundamental Principles of Mathematical Sciences. Springer, New York.

- Guckenheimer, J., Holmes, P., 1983. *Nonlinear Oscillations, Dynamical Systems, and Bifurcations of Vector Fields*, 2nd Edition. Applied Mathematical Sciences. Springer, New York.
- Hanski, I., 1998. Metapopulation dynamics. *Nature* 396, 41–49.
- Hanski, I., 1999. *Metapopulation Ecology*. Oxford University Press, Oxford.
- Hanski, I., Gyllenberg, M., 1993. Two general metapopulation models and the core-satellite species hypothesis. *Am. Nat.* 142, 17–41.
- Hanski, I., Ovaskainen, O., 2000. The metapopulation capacity of a fragmented landscape. *Nature* 404, 755–758.
- Harding, K. C., McNamara, J. M., 2002. A unifying framework for metapopulation dynamics. *Am. Nat.* 160, 173–185.
- Hui, C., Li, Z., 2004. Distribution patterns of metapopulation determined by allee effects. *Popul. Ecol.* 46, 55–63.
- Jagers, P., 1992. Stabilities and instabilities in population dynamics. *J. Appl. Prob.* 29, 770–780.
- Lande, R., Engen, S., Sæther, B.-E., 1998. Extinction times in finite metapopulation models with stochastic local dynamics. *Oikos* 83, 383–398.
- Levins, R., 1969. Some demographic and genetic consequences of environmental heterogeneity for biological control. *Bull. Entomol. Soc. Am.* 15, 237–240.
- Lopez, J., Pfister, C., 2001. Local population dynamics in metapopulation models: Implications for conservation. *Conserv. Biol.* 15, 1700–1709.
- Martcheva, M., Bolker, B. M., 2007. The impact of the allee effect in dispersal and patch-occupancy age on the dynamics of metapopulations. *B. Math. Biol.* 69, 135–156.
- Meerson, B., Sasorov, P. V., 2011. Extinction rates of established spatial populations. *Phys. Rev. E* 83, 011129.
- Mehlig, B., Wilkinson, M., 2007. Precise asymptotics for a variable-range hopping model. *Prog. Theor. Phys. Suppl.* 166, 136–142.

- Melbourne, B. A., Hastings, A., 2008. Extinction risk depends strongly on factors contributing to stochasticity. *Nature* 454, 100–103.
- Nachman, G., 2000. Effects of demographic parameters on metapopulation size and persistence: an analytical stochastic model. *Oikos* 91, 51–65.
- Roy, M., Harding, K., Holt, R.-D., 2008. Generalizing levins metapopulation model in explicit space: Models of intermediate complexity. *J. Theor. Biol.* 255, 152–161.
- Sæther, B.-E., Engen, S., Lande, R., Møller, A.-P., Bensch, S., Hasselquist, D., Beier, J., Leisler, B., 2004. Time to extinction in relation to mating system and type of density regulation in populations with two sexes. *J. Anim. Ecol.* 73, 925–934.
- Samuelson, P. A., 1977. Generalizing Fisher’s “reproductive value”: linear differential and difference equations of “dilute” biological systems. *Proc. Natl. Acad. Sci. USA* 74, 5189–5192.
- Schaper, E., Eriksson, A., Rafajlovic, M., Sagitov, S., Mehlig, B., 2012. Linkage disequilibrium under recurrent bottlenecks. *Genetics*, in press.
- Taylor, C., Hastings, A., 2005. Allee effects in biological invasions. *Ecol. Lett.* 8, 895–908.
- van Kampen, N. G., 1981. *Stochastic Processes in Physics and Chemistry*, 2nd Edition. North-Holland, Amsterdam.
- Wilkinson, M., Mehlig, B., Östlund, S., Duncan, K. P., 2007. Unmixing in random flows. *Phys. Fluids* 19, 113303.
- Zhou, S.-R., Liu, C.-Z., Wang, G., 2004. The competitive dynamics of metapopulations subject to the allee-like effect. *Theor. Popul. Biol.* 65, 29–37.
- Zhou, S.-R., Wang, G., 2004. Allee-like effects in metapopulation dynamics. *Math. Biosci.* 189, 103–113.

Figures

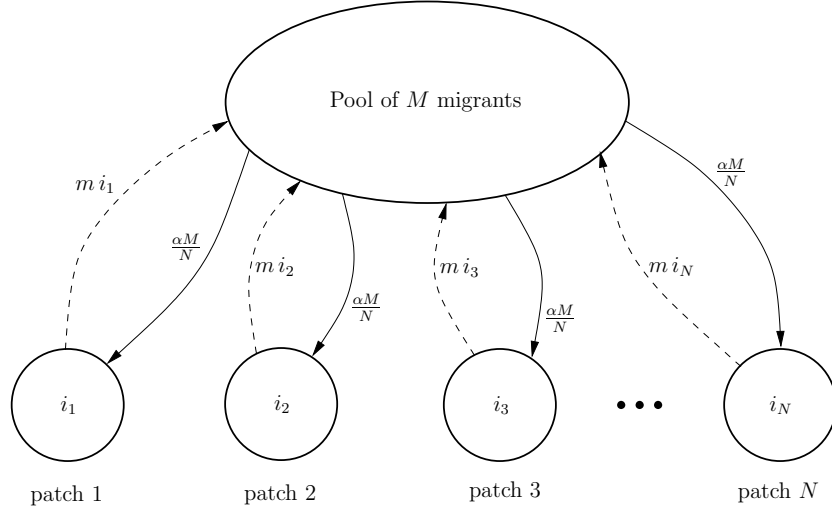


Figure 1: Illustration of the stochastic, individual-based meta-population model. The model describes N local populations (also referred to as patches). The number of individuals on path k is denoted by i_k . Individuals are born and die with rates per capita b_{i_k} and d_{i_k} . Furthermore, individuals may emigrate to a common dispersal pool (emigration rate m) where they stay an exponentially distributed time (with rate α) before leaving the pool for one of the N patches. Migration may fail if the individuals die before reaching the new patch, this possibility is modeled by a introducing a death rate ν during dispersal. The instantaneous number of migrants in the pool is denoted by M . The immigration rate from the dispersal pool into any given patch is given by $I = \alpha M/N$.

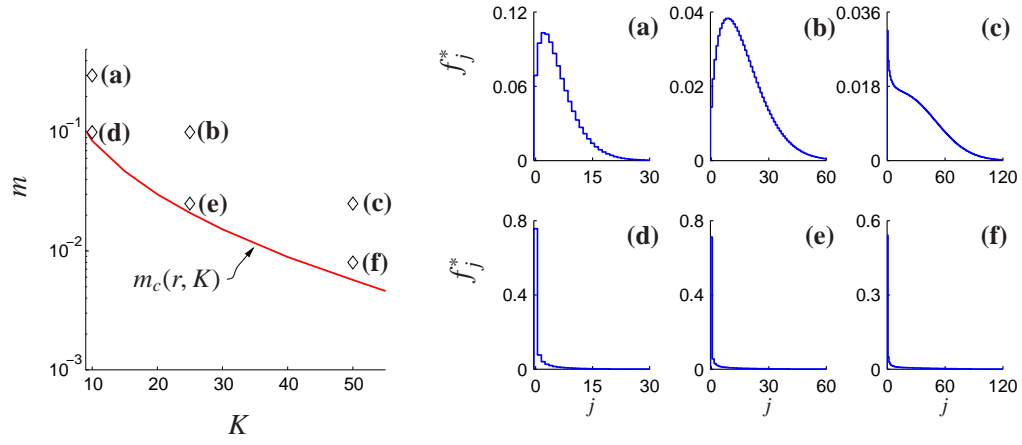


Figure 2: Left: critical migration rate m_c , computed from (33), as a function of the carrying capacity K (solid red line). The growth rate is $r = 1.05$. Above the red line, metapopulations persist in the limit of $N \rightarrow \infty$. Right: shows six different stable steady states f^* , obtained by solving Eqs. (29, 30) numerically, for $r = 1.05$ and the values of m and K indicated in the left panel.

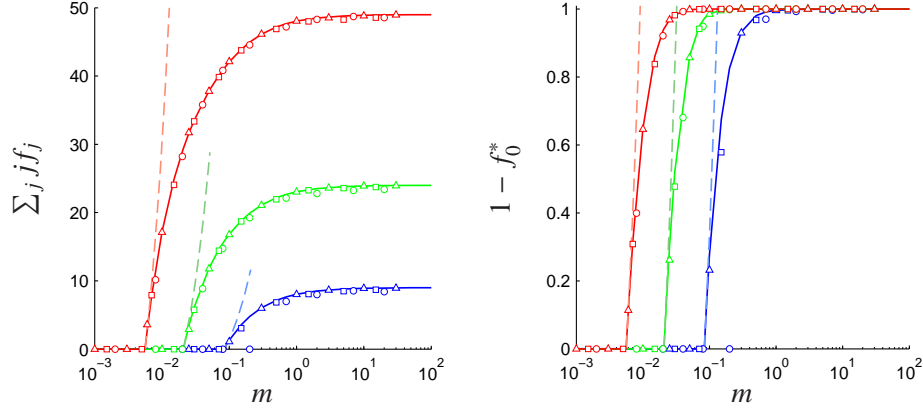


Figure 3: Left: average number of individuals per patch in the quasi-steady state as a function of the migration rate m . Shown are the numerical solution of Eqs. (15,17), solid lines. Parameters: $r = 1.05$, $K = 10$ (blue), $K = 25$ (green), and $K = 50$ (red). Curves corresponding to the asymptotic expression (36), valid as $m \rightarrow m_c$, are shown as dashed lines. Also shown are results of direct numerical simulations as described in section 2.2 for $N = 1000$ (Δ), $N = 100$ (\square), and $N = 50$ (\circ). Right: same but the fraction of occupied patches $1 - f_0^*$ as a function of m . The asymptotic behaviour as $m \rightarrow m_c$ is given by (35) (dashed lines). The results for the direct simulations were obtained as follows. For each set of parameters we performed 30 stochastic runs up to a time smaller than the expected time to extinction (if extinction occurred, the simulation was discarded). After the initial transient, 20 samples were taken from each simulation (separated by a time long enough so that the samples were uncorrelated). Thus each point is the average of 600 independent realisations. If the simulations consistently became extinct during the initial transient we concluded there was no quasi-steady state, and f_0^* was set to unity.

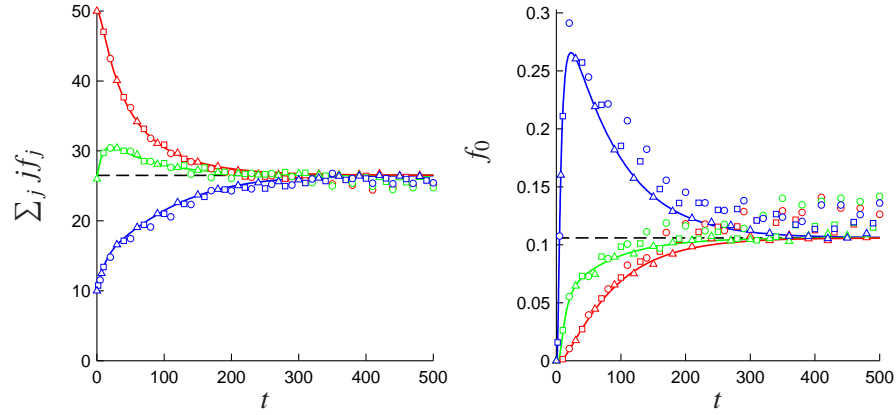


Figure 4: Left: average number of individuals per patch as a function of time for $r = 1.05$, $K = 50$, and $m = 0.0167$. Shown are numerical solutions of Eqs. (15,17) for three different initial conditions: five individuals per patch at $t = 0$ (blue solid line), 26 individuals per path (green) and 50 individuals per patch (red). Also shown are results of direct simulations as described in section 2.2, for $N = 1000$ (\triangle), $N = 100$ (\square) and $N = 50$ (\circ), for each of the three initial conditions. The steady-state value is shown as a black dashed line. Right: same, but f_0 as a function of time. Each point of the direct simulations corresponds to an average over 100 stochastic realisations conditional on no extinction (no extinction actually occurred during these simulations).

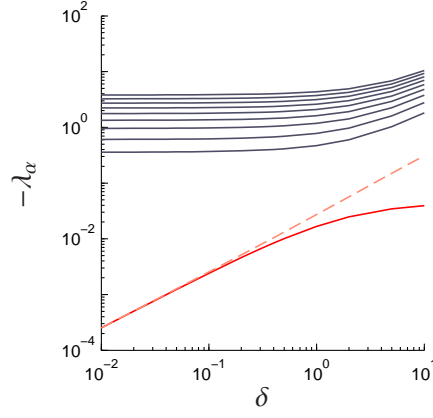


Figure 5: Shows $-\lambda_\alpha$ (where λ_α are the eigenvalues of \mathbf{A} at the steady state), for $\alpha = 1, \dots, 10$, $r = 1.05$, and $K = 10$, as a function of δ , obtained by numerically diagonalising the matrix (A.2) truncated at $j = 120$. The largest eigenvalue λ_1 is shown in red. The dashed line corresponds to $\langle L_1 | \mathbf{A} | R_1 \rangle$, where $\langle L_1 |$ and $| R_1 \rangle$ are evaluated at the bifurcation, while \mathbf{A} is evaluated at the steady state corresponding to the value of δ chosen.

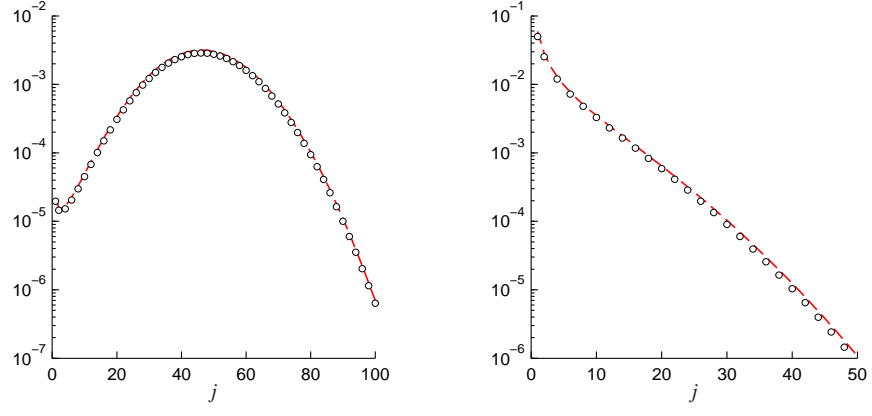


Figure 6: Shows $|R_1\rangle Q_1^*$ (dashed lines), compared to $|f^*\rangle$ (\circ) for $\delta = 0.1$. Parameters: $r = 1.5$, $K = 50$ (left) and $r = 1.05$, $K = 10$ (right).

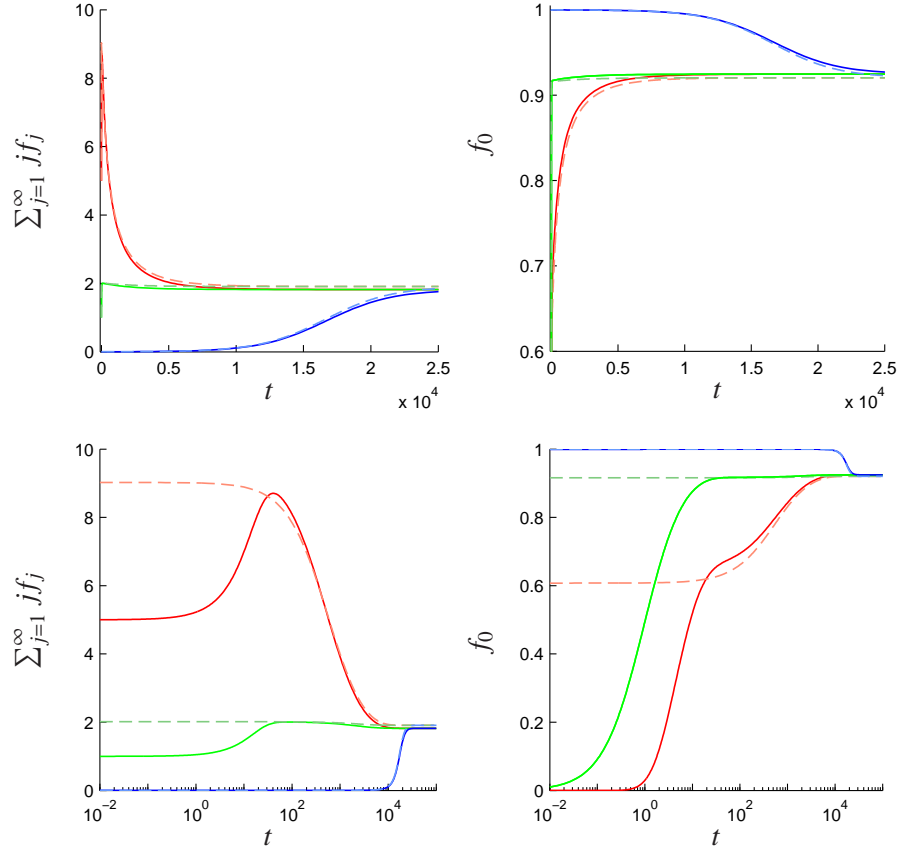


Figure 7: Deterministic relaxation towards the stable steady state \mathbf{f}^* . Top left: average number of individuals per patch, $\sum_{j=1}^{\infty} j f_j$ as a function of time for $r = 1.05$, $K = 50$, and $\delta = 0.05$. Shown are numerical solutions of Eqs. (15,17) for three different initial conditions: five individuals per patch at $t = 0$ (red solid line), 1 individuals per patch (green) and expected number of individuals per patch equal to 10^{-3} (blue). Also shown are solutions of Eqs. (42) and (45) (dashed lines). Top right: same, but f_0 as a function of time. Bottom: same as above, but on a logarithmic time scale.

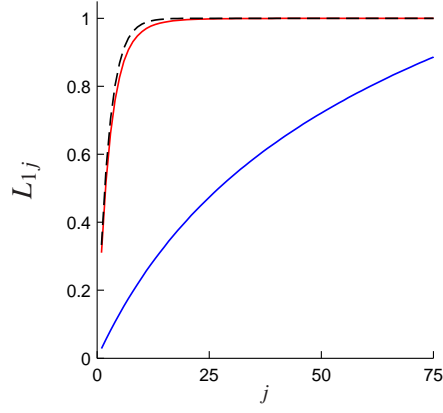


Figure 8: Shows the components of $\langle L_1 |$, L_{1j} , as a function of j , for $r = 1.5$, $K = 50$ (solid red line), and for $r = 1.05$, $K = 10$ (solid blue line). The dashed line corresponds to (50), evaluated for $r = 1.5$.

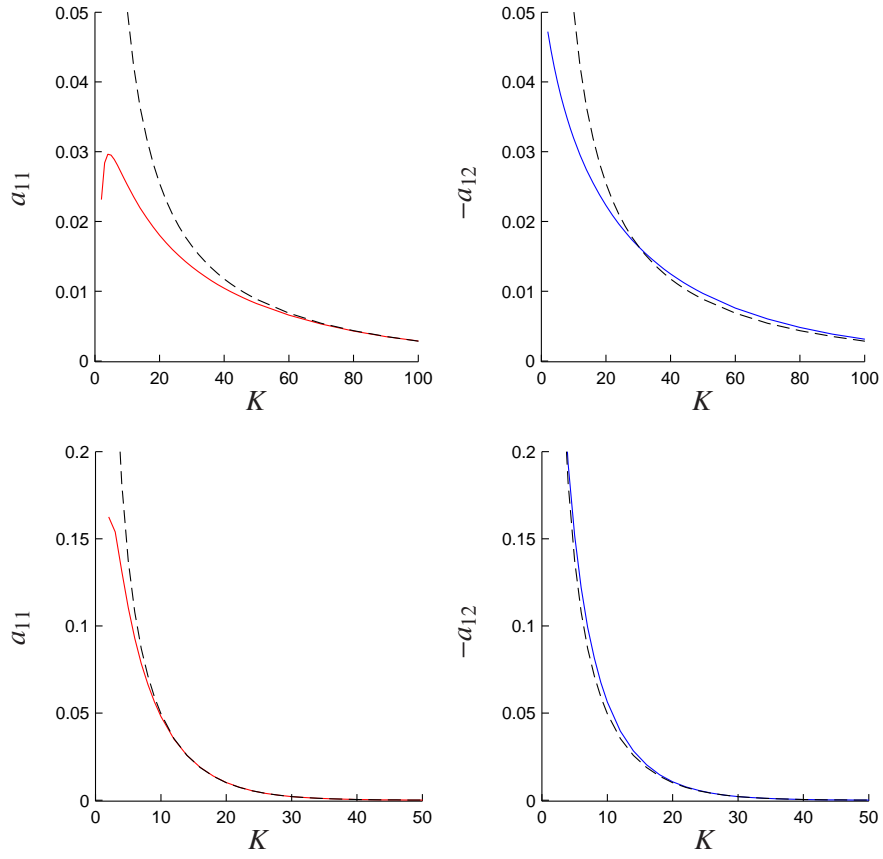


Figure 9: Shows the rates a_{11} (solid red lines) a_{12} (solid blue lines), given by Eqs. (B.8,B.9) in appendix B, depend upon the carrying capacity K for $r = 1.05$ (upper panels) and $r = 1.5$ (lower panels). Also shown (dashed black lines) the asymptotic law for large values of K , Eq. (53).

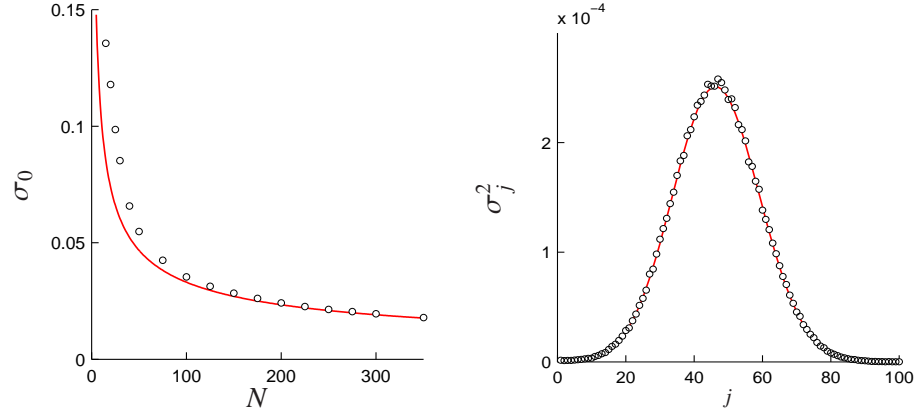


Figure 10: Left: standard deviation of f_0 as a function of the number of patches N . Comparison of σ_0 , calculated from from \mathbf{C} in (28) and employing (54) (solid red line), to direct numerical simulations (\circ). The agreement is very good for N of the order of 100. Parameters: $r = 1.05$, $K = 50$, $m = 0.02$. Right: comparison of the variances σ_j^2 , calculated using (28) (solid red line), to direct numerical simulations (\circ) for $N = 100$. Parameters: $r = 1.5$, $K = 50$, $m = 2.5 \times 10^{-5}$.

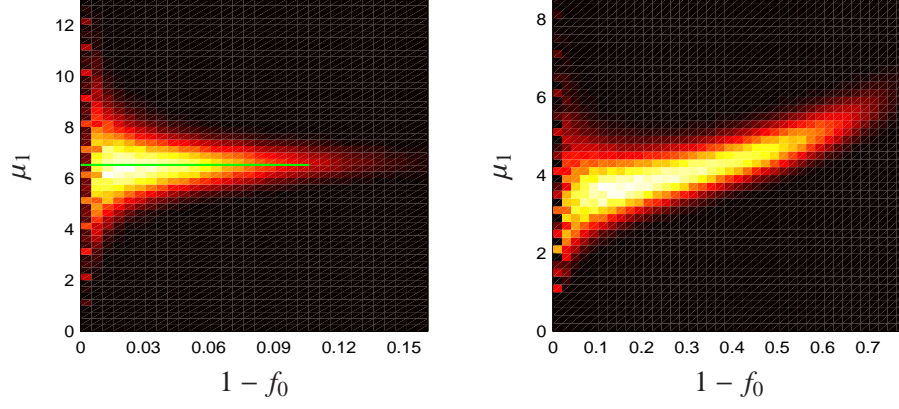


Figure 11: Results of direct numerical simulations of the stochastic, individual-based model, determining the most likely path to extinction. Shown is the distribution of the number of individuals on occupied patches $\mu_1 = \sum_{j=1} j f_j / \sum_{j=1} f_j$ conditional on the number of occupied patches. Parameters: $r = 1.5$, $K = 10$, $\delta = 0.1$, $N = 1000$ (left) and $r = 1.05$, $K = 10$, $\delta = 0.61$, and $N = 250$ (right). The probability is colour coded: high probability corresponds to white, low probability to black. How this plot was produced is described in the text. Also shown (only in the left panel) is the result of the slow dynamics given by Eqs. (51), (67), and (69) (solid green line).

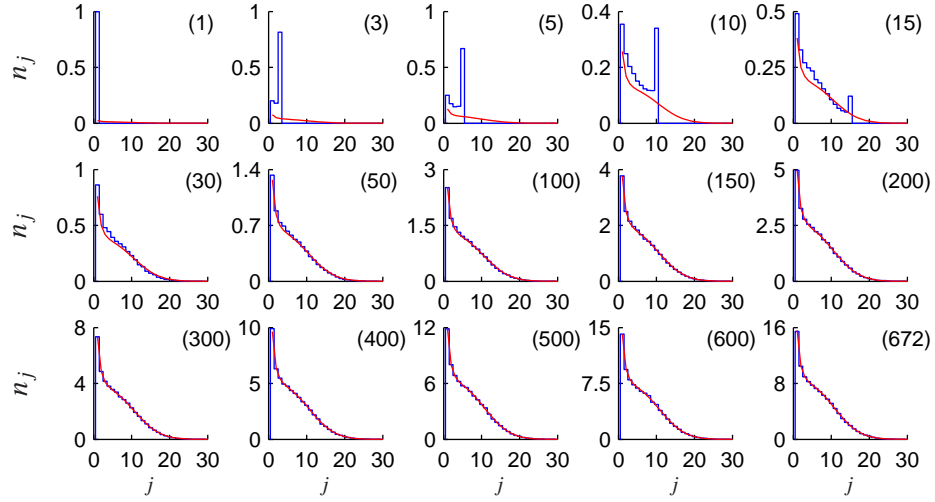


Figure 12: Each panel shows the n_j -spectrum conditional on that there are (n) individuals in the metapopulation. Thus the upper-leftmost panel shows the n_j -spectrum conditional on that there is one individual, and the lower-rightmost panel corresponds to 672 individuals (the expected number of individuals at the steady state). Results from direct simulations (averaged over 10^4 stochastic realisations) (blue) are compared to the numerical integration of the Hamiltonian dynamics (20,21) (red). Parameters: $r = 1.5$, $K = 10$, $\delta = 0.103$, $N = 1000$. Note that the first value of j in each panel is 1 (n_0 is not plotted).

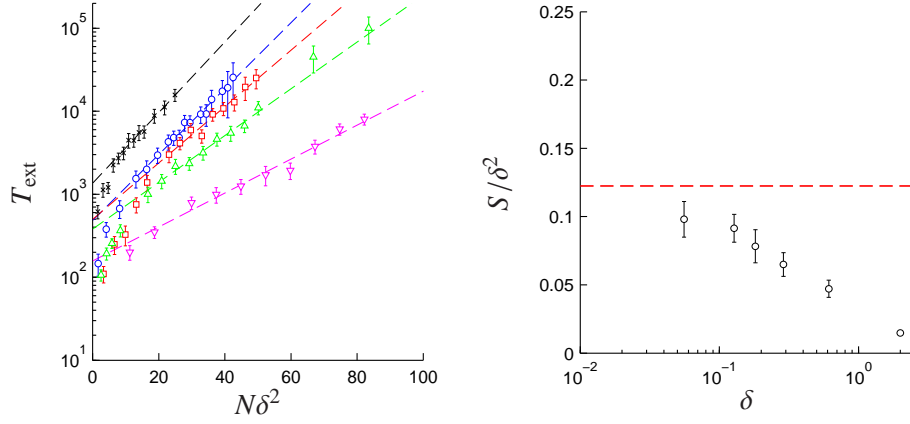


Figure 13: Left: average time to extinction T_{ext} from direct numerical simulations of the model described in section 2.1, as a function of the number of patches N , for $r = 1.05$, $K = 10$. Symbols (black to magenta) correspond to the following values of δ : 0.0557, 0.128, 0.182, 0.289, 0.611. Each point corresponds to an average over 100 stochastic realisations. Also shown are numerical fits to the expected behaviour (70). Right: action as a function of δ . Shown are the analytically determined action limit (71) (dashed red line), as well as the results of the fits shown in from the left panel (\circ). Error bars correspond to 95% confidence intervals.

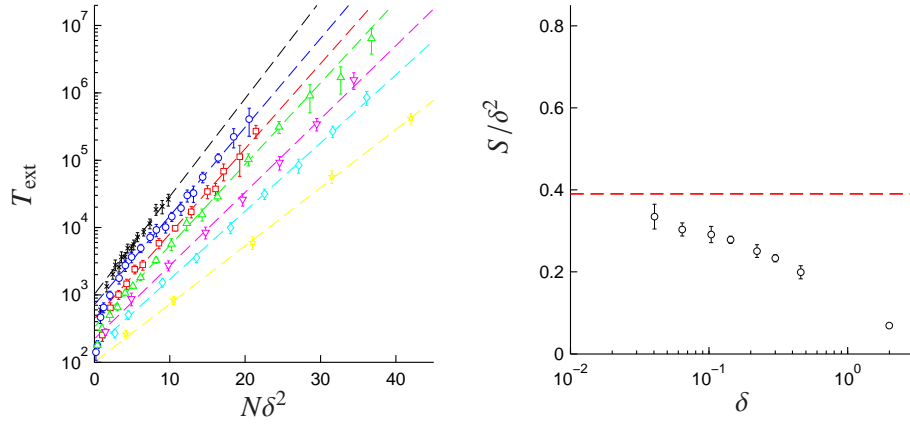


Figure 14: Same as Fig. 13, but for $r = 1.5$ and $K = 10$. The symbols (black, blue, red, ... , yellow) correspond to $\delta = 0.04, 0.064, 0.103, 0.143, 0.222, 0.301$, and 0.458 .

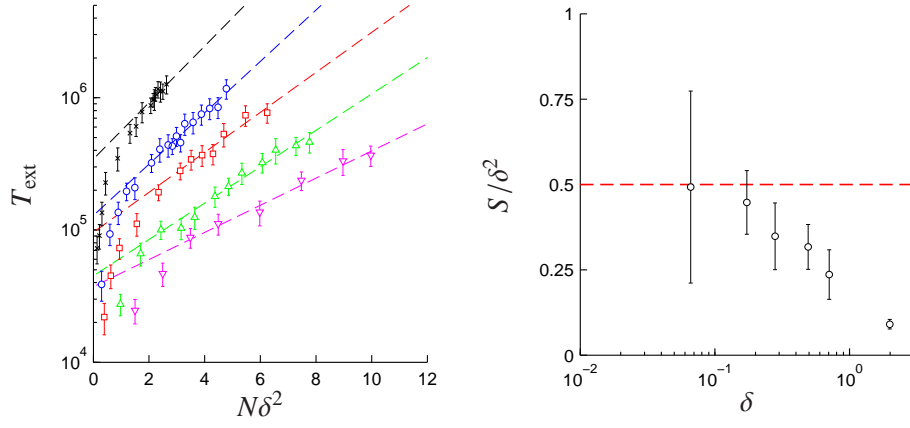


Figure 15: Same as Figs. 13 and 14, but for $r = 1.5$ and $K = 50$. Black, blue, red, green, and magenta symbols correspond to $\delta = 0.066, 0.173, 0.279, 0.493$, and 0.706 .

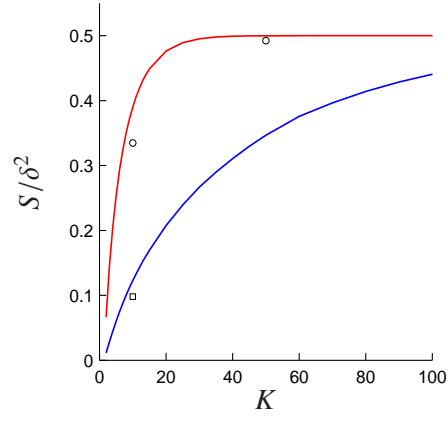


Figure 16: S/δ^2 according to Eq. (71), in the limit of $\delta \rightarrow 0$, as a function of K . Blue and red solid lines correspond to $r = 1.05$ and 1.5 , respectively. Symbols correspond to the best estimates from Figs. 13 to 15.

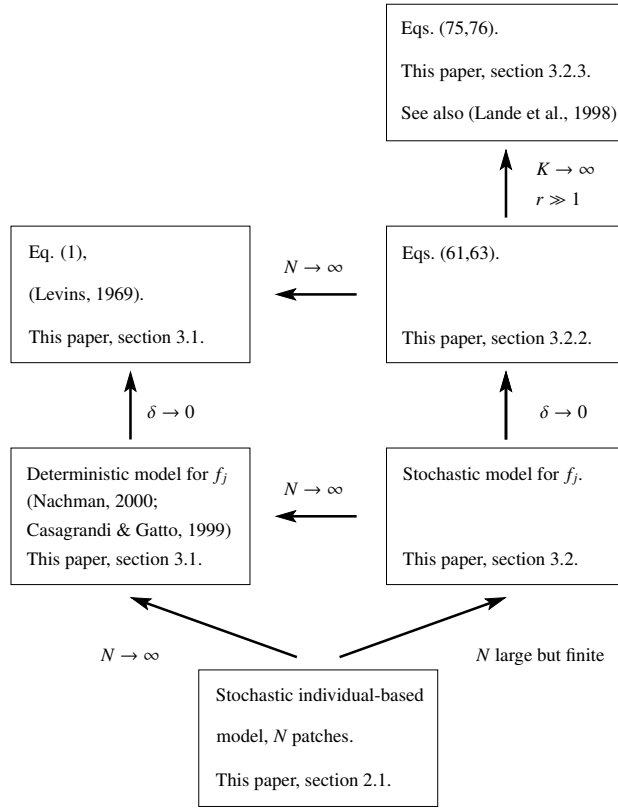


Figure 17: Schematic diagram showing relations between different limiting cases of the individual-based stochastic metapopulation model described in section 2.1.